Improving Indoor BlueTooth Localization by Using Bayesian Reasoning to Explore System Parameters

A Thesis Submitted to the
College of Graduate Studies and Research
in Partial Fulfillment of the Requirements
for the degree of Master of Science
in the Department of Computer Science
University of Saskatchewan
Saskatoon

By
Gregory Scott Johnston

Permission to Use

In presenting this thesis in partial fulfilment of the requirements for a Postgraduate degree from the University of Saskatchewan, I agree that the Libraries of this University may make it freely available for inspection. I further agree that permission for copying of this thesis in any manner, in whole or in part, for scholarly purposes may be granted by the professor or professors who supervised my thesis work or, in their absence, by the Head of the Department or the Dean of the College in which my thesis work was done. It is understood that any copying or publication or use of this thesis or parts thereof for financial gain shall not be allowed without my written permission. It is also understood that due recognition shall be given to me and to the University of Saskatchewan in any scholarly use which may be made of any material in my thesis.

Requests for permission to copy or to make other use of material in this thesis in whole or part should be addressed to:

Head of the Department of Computer Science
176 Thorvaldson Building
110 Science Place
University of Saskatchewan
Saskatoon, Saskatchewan
Canada
S7N 5C9

Abstract

With the advent of smaller, more mobile electronic devices, a wide variety of services can now be augmented with the additional context that is provided by positional information. Systems commonly used for outdoor localization, such as GPS, cannot necessarily be used for indoor localization because often, separating a localizing device from system infrastructure with walls and other obstacles lowers accuracy. Instead, indoor localization systems can be deployed to replace the contextual information required for some situated services, that would otherwise be lost when a device moves indoors.

For example, the trilateration algorithm that GPS uses to combine distance estimates from satellites can be repeated using Bluetooth (BT) devices spread throughout an environment. The signal strength of a set of beacons can be read by a localizing device, and those signal strengths can be equated to the distance between the localizing device and the beacon. These distances can then be combined using trilateration.

A major source of error in such a system is that BT signal strength does not map directly to only one distance. Because microwave frequency propagation is susceptible to multipath effects and antenna direction, two devices at a fixed location can read a variety of signal strengths, which may not map to the ideal line-of-sight calibrated value. Therefore, any given signal strength reading cannot be interpreted as a single distance without introducing the potential for substantial error.

One solution is to probabilistically model the relationship between distance and signal strength by modelling BT localization using a Bayesian network. In a Bayesian network, the distance versus signal strength relationship is stored as the conditional probability of a signal strength reading given a specific distance. Using a Bayesian inference algorithm, one can then reason backwards from a signal strength to a probability distribution representing the estimated position of the localizing BT device.

In this thesis, I explore some of the effects of modelling BT localization with a Bayesian network. I first extend the probabilistic calibration to include the influence of the relative orientation of device antennae on the attenuation of BT signal strength between them. I then experiment with the effects of the position of a receiver within a discrete spatial bin,

and of the proximity of the transmitters to the edges of the discrete space, because both have the potential to reduce the accuracy of localization using discrete variables. I found that neither affected the localization results in a significant, avoidable fashion. I then studied the effects of the scope of calibration, in terms of the number of distance values used, and of the number of beacons used in localization. I found that additional distance values and a smaller minimum distance used in calibration could result in increased BT localization accuracy, whereas many BT localization systems perform little calibration at distances smaller than 2 m. I also found that accuracy increased when the number of beacons was greater than four, and that accuracy did not significantly decrease when the number of beacons was three or fewer; whereas most trilateration systems use only three or four beacons. I conclude in general that a combination of probabilistic trilateration calibration and Bayesian network inference are viable techniques, and could allow for improvements to localization accuracy in a number of areas.

Acknowledgements

I would like in particular to thank my supervisors Mike Horsch and Kevin Stanley for their guidance and instruction throughout the span of my Master's program.

I would also like to thank Christopher Brooks, Mike Bullock, Wook Jung, Greg Logan, Craig Thompson, Jiajing Wang, and Ting Wei, for their help in performing some of the data collection procedures described in this thesis document; as well as the IT staff of the University of Saskatchewan's Computer Science Department for their help and support in gathering and deploying the hardware used in the same procedures.

I would also like to thank my family for being understanding when I disappeared without contact into my work for weeks at a time, and my friends for enticing me out of the house from time to time.

"What the strag will think is that any man who can hitch the length and breadth of the galaxy, rough it, slum it, struggle against terrible odds, win through, and still know where his towel is, is clearly a man to be reckoned with."

– Douglas Adams, *Hitchhiker's Guide to the Galaxy*

Contents

List of Tables

List of Figures

List of Abbreviations

BT	BlueTooth
CDF	Cumulative Distribution Function
CPT	Conditional Probability Table
DAG	Directed Acyclic Graph
GPS	Global Positioning System
HMM	Hidden Markov Model
MAC	Media Access Control
RAM	Random Access Memory
RFEM	Radio-frequency electromagnetic
RFID	Radio-frequency identification
RSSI	Received Signal Strength Indicator
WLAN	Wireless Local Area Network

Chapter 1

Introduction

The vast majority of computation undertaken by humanity is abstract enough that most applications and theory in the field of Computer Science are independent of the computing device's current position. On the other hand, situated computation has grown recently, as the number of possible applications that require positional knowledge has increased. From broad networks of mobile sensors deployed across a city [22], to more personalized services such as map-based navigation systems,[1] location-based social networking tools,[2] and augmented reality applications,[3] the additional context of where a computation is being performed has become important as the miniaturization of electronics has marched on, making technology more and more ubiquitous.

Existing applications that use a device's position to improve services are as varied as: finding co-workers in an office environment; guiding visitors between key locations in a museum, with instructions from a PDA; or as "support services for individuals who have wayfinding difficulties due for example to low vision, stroke, and traumatic brain injury" [51]. Often, the devices will be mobile because of their attachment to people, such as in the case of a mobile phone. But just as easily, the device could be a mobile robot attempting to position itself indoors [48, 49]; or even devices attached to cows in a barn, placed there to monitor the cows' behaviour and hopefully allow farmers to preemptively detect disease [50]. Some potential applications in the literature might be described as futuristic. For example, a person's situation could be determined from their personal mobile device and used to influence other devices around them:

"Let us consider a simple ubiquitous computing scenario. Alice enters a room

[1] `http://maps.google.com`
[2] `http://foursquare.com`
[3] `http://www.layar.com`

> while communicating with a colleague by cellular phone. The colleague (Bob) is sitting in the lab in front of a fully equipped video conferencing system, using voice over IP to reach Alice's cellular phone. When Alice enters the room, she is faced with a network television system with greater communication abilities. The system thus automatically, in accordance with Alice's selected preferences, changes her communication session to the TV display system, and launches video conferencing." [6]

Other possibilities include:

> "[. . .] the location detection of products stored in a warehouse, location detection of medical personnel or equipment in a hospital, location detection of firemen in a building on fire, detecting the location of police dogs trained to find explosives in a building, and finding tagged maintenance tools and equipment scattered all over a plant." [30]

As accurate position information continues to be made more available to software engineers and developers, the tools to take advantage of positioning information in these ways will likely grow in turn.

The general problem faced in implementing these types of services is localization: finding a device's position in the real world. The Global Positioning System (GPS) is the most widely recognized example of a localization system. GPS's positioning uses estimates of distance based on the time of flight of electromagnetic waves between the system's satellites and the localizing device. There are also variations of GPS that make use of the same set of satellites: Differential GPS, where the position of a user's GPS device is measured relative to another GPS device that is more accurately localizable by GPS, rather than localizing relative to the satellite system itself [7]; and Assisted GPS, where an overlapping network of ground-based antennae broadcast the handshaking data that would otherwise be received only from the satellites before localization [33]. Both of these can improve the speed and accuracy of localization. There are also "cell-of-origin" methods for mobile phones that work on the same principles of distance estimation from known locations, but that eschew GPS satellites and localize based on proximity to cellphone towers [7]. Other lesser-known systems include the VHF Omnidirectional Ranging system, which is also based on the same principles but with different signals used for range estimation, and used for localizing airplanes for navigation [24]. Localization can also be performed using TV transmission signals for ranging data [37].

However, for GPS to maintain its accuracy, a device requires line-of-sight contact with at least four of the system's satellites, because GPS uses the time of flight of signals between the satellites and localizing device. When the signal travels through structural barriers such as roofs and walls, it can be impeded, reflected, or even completely absorbed, changing the time of flight and therefore the estimated distance between the device and the satellites [7]. This means that the observed accuracy of GPS often decreases once a device is indoors. An alternative to using GPS for indoor applications is to repeat the structure and function of GPS's array of satellites with Wireless Local Area Network (WLAN) or Bluetooth (BT) nodes distributed through the environment [24, 7, 33, 30, 51]. As well, Radio-Frequency Identification (RFID) tags are small enough that they can be placed on products in a warehouse or store and used to localize them [27], or to localize customers to within an aisle of a store [30].

Both BT and WLAN devices transmit data using microwaves in the 2.4 GHz band; as well, both are present in a wide range of consumer electronic devices. This ubiquity means that BT and WLAN beacons are both good potential candidates to replace GPS satellites for indoor localization. However, BT has a number of benefits over WLAN for indoor localization. BT is designed to be a lower-powered communication option over short ranges. Because it uses less power, it can be more efficient for an indoor localization system to use BT beacons, in terms of energy usage; if the devices are battery-powered, this will also reduce the amount of time spent changing batteries. BT's short range also affects the resolution of indoor localization. The Received Signal Strength Indicator (RSSI) used to measure signal strength is reported by both BT and WLAN receivers in integer increments, but because the useable range of RSSIs for BT occurs on a shorter range of distances, an integer change in RSSI translates to a smaller change of distance for BT than for WLAN. Although devices in a BT localization system have to be within the effective 10 m range of BT, the smaller change in distance per change in RSSI value can result in a finer-grained resolution.

My objective in this thesis work is to examine the problems and limitations to opportunistically measuring distances from coincidental contact with BT devices extant in the environment; and to provide generalizable conclusions about the effects of certain parameters on the accuracy of trilateration-based systems. Specifically, I use iMacs in this thesis document as examples of devices that might be found naturally in an indoor setting. Some of

the technical details of indoor localization with BT are described in Chapter 2. In Chapter 3, I present my model of BT localization when using iMacs as beacons. The model is built as a Bayesian network with discrete variables; the fundamentals of Bayesian networks is described in §3.1, followed by the specifics of my model in §3.2–3.5.

Although studies have been done on the accuracy of BT localization with variations on the standard localization algorithms of fingerprinting (§2.1) or trilateration (§2.2), no known studies have adequately examined the effects of specific implementational parameters on accuracy. In Chapter 4, I present the methods and results of a variety of experiments that test how distance calibration (§4.5.1) and the number of beacons (§4.5.2) can affect the accuracy of BT localization.

When I added distance values to my model, I found an increase in the accuracy of repeated simulations of localization over that found when the associated calibration data was not used. I therefore conclude that using additional distance calibration levels has the potential to increase the accuracy of indoor BT localization. I also repeated localization simulations using from 1 through 8 BT beacons, and saw the accuracy of localization increase with more beacons than four, but not significantly decrease with fewer beacons than three. From the results of this experiment, I conclude that having more beacons than the traditional four has the potential to increase the accuracy of indoor BT localization; but that having only two beacons does not significantly decrease the accuracy of localization. Based on these results, I discuss future possibilities for the model and for iMac localization in §5.4.

Chapter 2

Localization Background

Localization can be broadly defined as the problem of determining a person or object's relative position with respect to some known coordinate system. GPS, for example, describes the position of a person or device in terms of global latitude and longitude coordinates [7]. For indoor localization where systems like GPS are less accurate, positions are more easily measured relative to a known map of the room, building, or buildings where devices are intended to be localized; occasionally, indoor localization determines global coordinates and translates to a local map [24]. The requirement of localizing a device relative to real world artifacts means that indoor positioning often requires two distinct sets of devices. The first is the device or devices with no known position, which I will refer to as the localizing device(s). The second set of devices I will refer to as beacons, or beaconing devices: they exist at known, fixed locations throughout the environment. By determining a localizing device's position relative to these stationary devices, one has then also determined the localizing device's position relative to a fixed external coordinate frame. More importantly, this requirement of fixed beacons in the environment means that for most indoor localization systems, a training or calibration phase is performed to gather information of how BT behaves in the intended localization environment, which is then followed separately by the actual localization phase. Calibration allows the localization system to interpret gathered signal strengths and translate them into information about the device's position. Examples of algorithms for performing this translation include: through a form of lookup-table that equates observations about the environment with known positions in the environment (known as fingerprinting); or through geometric calculations based on fixed beacon locations and a localizing device's angles (triangulation) or distances (trilateration) relative to them. Methods of BT localization can therefore be loosely categorized based on the type of training phase they use, described in

§2.1 and §2.2, respectively. In §2.3, I discuss the variety of exceptions to this categorization.

It is worth clarifying terminology discrepancies in the literature. The first is the difference between "anchors," "beacons," "devices," and "nodes." The terms "device" [1, 2, 3, 4, 11, 14, 15, 16, 17, 20, 23, 26, 30, 32, 36, 38] and "node" [1, 2, 9, 16, 17, 28, 40] are used interchangeably as generic terms for something that contains a BT or WLAN transceiver; in this thesis document, I will exclusively use the term "device" for a generic BT entity in the localization environment. The term "beacon" [11, 15, 20, 23, 38, 40] is derived from the fact that BT has a "discoverable" mode where a device broadcasts that it is available for connections. The term "anchor" is used mostly in the sensor network localization subfield [31, 34, 47], to denote the fact that in a sensor network, there is a number of devices to localize, and a smaller number that are fixed or anchored in space, to which relative locations are determined; it is only seldom used outside of the area of sensor networks [9].

The second terminology discrepancy is between the application of terms such as beacon or node to individual devices within a localization system. The distinction between localizing devices and beaconing devices is a broad categorization that will be used in this thesis document, but it does not precisely apply to every localization system. The term "localizing device" assigns an agency to the device with unknown location, but many localization systems involve a centralized server that performs the localization algorithms and merely reports the device's location to it over a network connection. In some cases the "beacons" do not perform any beaconing, where instead the broadcasting of discoverability is done by the device with unknown location, while the devices with fixed locations combine their observed information about the unfixed device through a network connection, and are the ones performing localization. This type of system is referred to as "network-based" by Pandey and Agarwal [33]. As well, Smith et al. used the Cricket localization system to compare both versions and a hybrid combination of the two, using sonar data to produce distance estimates between devices. They refer to the network-based system of Pandey and Agarwal as an "active" system because it is the localizing device that actively beacons; and a system where the localizing device is gathering beacon data, they refer to as "passive" [46]. The distinction is worth mentioning here for completeness only: the system described in this thesis document represents one localizing device that records signal strengths from stationary, beaconing de-

vices. For the rest of this document, I will not make a distinction between active, passive, and network-based systems when I am describing them, because such a description would not help make the system's relevance to this work any clearer. Instead I will always refer to any system as though it were passive, so that every description uses the same terminology as the work described in this document.

2.1 Fingerprinting

Fingerprinting is a class of BT localization methods that attempt to determine the position of a localizing device by recognizing BT signal strengths that are known to be characteristic of specific locations. For example, the simplest possible fingerprinting system would place one BT beacon in each room of a building, and then simply conclude that if at any time a localizing device receives higher signal strength readings from the beacon corresponding to one room than any other, then the localizing device must be closest to that beacon and therefore is in that beacon's room. More generally, the training phase of a fingerprinting system involves actively traversing the entirety of the intended localization environment, and gathering characteristic BT measurements of every possible position. The localization phase is to then gather current data, and approximately match that data to the "fingerprint" of known locations.

Assuming that a fingerprinting system can develop a mapping with a unique pattern of signal strengths for each possible location, this type of localization can be quite accurate. In the simple example mentioned in the preceding paragraph, it is highly unlikely for a localizing device to read a higher signal strength from a device in the next room than from the device in the same room. However, what fingerprinting might gain in accuracy by localizing a device in the correct room, it can easily lack in resolution. In the previous example with only one beacon per room, the most exact that a resulting position estimate can be is to say that the device is somewhere within that room. Although for some applications this is a perfectly acceptable lower bound on resolution, for many applications, it is not. For example, the knowledge that a cow is in a barn does not necessarily allow a farmer or veterinarian to draw any additional conclusions about its behaviour.

A good example of a fingerprinting technique that has a broad resolution is that proposed by Filho et al. [16]. In their localization system, they divide the map of the localization environment into "regions of confidence" based on the probability of observing the discoverability announcement of a beacon. This probability is measured in the training phase, where in advance, a BT device is moved throughout the space, making a connection inquiry to every BT beacon in the system that it can reach. At any location, there is a certain probability that a localizing device's inquiry will be responded to by a given beacon. Locations are said to be in a beacon's region when that probability is above a certain threshold. Regions are further subdivided into "sectors," which are all the possible combinations of known regions. In the localizing phase, the localizing device attempts again to make connection inquiries to beacons in the system, and the device is localized to whatever sector its current readings match. However, the sectors found in Filho et al.'s implementation spanned whole rooms up to 10m^2 in area. Although this is an acceptable resolution for certain applications, it does not lend itself easily to a measure of accuracy: the question it asks is less of the form "where am I?", which can be evaluated using a Euclidean distance; instead the question is closer to "what room am I in?", whose accuracy can only be measured as true or false. A resolution of 10m^2 is roughly equal to the useful precision of GPS indoors.

Aparicio et al. [3, 4] also use a fingerprinting method that combines overlapping regions, that they refer to as cells. However, their system differs from that of Filho et al. by incorporating signal strength readings from Wi-Fi routers in the environment. Other fingerprinting systems might use more complicated methods for mapping signal strength readings to location, such as in Roos et al. [39] and Pei et al. [36]. They represent the problem of localization as a machine learning task, where the mapping from readings in the environment to location in the environment is in the form of classification to match the histogram of observations recorded live with one of a set of known histograms recorded as training. Other BT localization systems that fall into the category of fingerprinting-based calibration include that of Hay and Harle [23], who experiment with connection-based metrics for distance estimation, such as the amount of data that can be transmitted reliably through a BT connection. Bahl and Padmanabhan [5] developed the fingerprinting-based system called RADAR, possibly one of the earliest BT localization systems.

Another important way that Aparicio et al.'s cell-based approach can be differentiated from Filho et al.'s is in the resolution of the system. Their cells are organized such that the possible places a device could be localized to are fixed points on a 2m grid. However, their system cannot escape the inherent cost of a fingerprinting-based system that for every point on their 2m grid, they had to perform a calibration step of recording signal strength readings at that point, and for long enough to avoid the sampling error inherent to instantaneous BT signal strength readings. Although fingerprinting methods can be straightforward to implement, there will always be this high cost of calibration effort to increase resolution, accuracy, and the scope and size of the localization space.

2.2 Trilateration

Trilateration is a prevalent alternative to fingerprinting techniques. A general definition of trilateration is localization using measured distances from known beacons or positions. With a system of equations of the form

$$r_i = \sqrt{(\boldsymbol{x}_i - \boldsymbol{x})^2} \tag{2.1}$$

where $\boldsymbol{x}$ is the position vector of a localizing device and $\boldsymbol{x}_i$ is the position vector of one beacon i, the set of r_i's is subsequently the Euclidean distance between the localizing device and a set of beacons. In a localization system, then, $\boldsymbol{x}$ is unknown, and to localize is simply to solve the system of equations for the localizing device's position. If the spatial vectors $\boldsymbol{x}$ and $\boldsymbol{x}_i$ have d spatial dimensions, then $d + 1$ equations are needed to uniquely determine a solution for $\boldsymbol{x}$. This is roughly how GPS determines location, using time of flight for signal transmission to estimate the distance of a device from GPS satellites' known locations.

In a BT system, distances are determined based on some measure of connectivity between BT devices. Agostaro et al. [1] explored using link quality to estimate distance: link quality is a measure present in the BT protocol for determining the amount of errors in the data stream between devices, which increases proportionally with distance. However, the most common way of determining distance is to equate signal strength loss, measured using RSSI, with the distance required to dissipate the measured signal. The defining reason for classifying

trilateration as distinct from fingerprinting, then, is that there is a direct translation from a single RSSI reading to a specific distance from an object in the environment, through which one can calculate a position in the environment; whereas fingerprinting is a mapping from a set of RSSI readings directly to an area in the environment.

RSSI can be equated to distance using an equation of the form

$$s_i = a - b \log r_i \tag{2.2}$$

where s_i is the measured signal strength from beacon i, and r_i is the distance of beacon i to the localizing device [12, 14, 28]. The parameters a and b are calibration constants that are determined in the preparation phase; after taking signal strength measurements at a variety of distances, they can be determined using standard regression techniques. This is why calibration for trilateration is in general less expensive, in terms of time and effort, than calibrating a fingerprinting system: instead of measuring signal strengths everywhere throughout the localization environment, signal strengths are measured once at a range of distances to produce calibration constants that are assumed to be consistent throughout the environment.

This system of equations is equivalent to the set of geometric equations that describes circles centred at the beacons. With three beacons, there are three equations, and thus three circles surrounding the beacons. When these three circles intersect at exactly one point (the position of the localizing device), the equations exactly define three radii r_i for these circles. The problem with a single, static calibration equation as in eq. 2.2, coupled with an attempt to determine the single intersection point of these circles, is that the wireless signal propagation of BT systems is inherently noisy, and prone to instantaneous error. Although in the real world, there is a single point at which the localizing device exists, if there is a signal error of even a few RSSI from one beacon, suddenly there may be no real-valued solution that satisfies the whole system of equations: the three circles might only intersect two at a time, rather than all three intersecting at one point. Resolving a most likely position from a set of equations with no unique solution is difficult, but possible: Gwon et al. [20] classify the possible intersections of circles into three common classes, and one rare class of intersections made up of five rare subclasses. They then determine a "region of confidence"

for the location of the device, based on each class's characteristic number of real-valued and imaginary-valued solutions. Although the difficulty of choosing a single, most likely position can be compensated for in a working system, it is never entirely overcome, as variations in signal strength are inherent in wireless communications.

Feldmann et al. [14] experimented with a variety of calibration equations, with limited success. The forms of equations they list in their paper are

$$s_i = c_0 \ln r_i + c_1 \tag{2.3}$$

$$s_i = c_0 + c_1 r_i + c_2 r_i^2 \tag{2.4}$$

$$s_i = c_0 + c_1 r_i + c_2 r_i^2 + c_3 r_i^3, \tag{2.5}$$

where c_0, c_1, c_2, and c_3 are their calibration constants. However, none of these four equation forms account for the observation that beyond seven meters, the possible RSSI cover a range of distances, rather than displaying a single value for a single distance [2, 14, 17, 32, 38]. Kotanen et al. [26] use a calibration equation with five additional terms, representing constant values such as the power levels of the receiving and transmitting antennae. The problem with such a system is that these measurements require the devices to have an active BT data connection between them, which can be costly to establish in terms of how much time it adds to the process of observing one distance measurement. In a system where the localizing device's position isn't merely unknown but is changing dramatically relative to the time scale of the system, requiring that the devices establish an active BT connection can be prohibitively time consuming. Agostaro et al. [1], as mentioned, use link quality as a measurement for distance, which also requires an active connection between devices. But in general, such measurements are not favoured because of the added time required.

One system with a unique approach to calibration is that of Fernández et al. [15]. They dynamically adjust their calibration parameters to account for changes in the environment, such as people moving through the room. To do this, they continuously take signal strength readings between the beacons. They then use these new readings in a model of the error between the actual, known distance, and a distance estimate that uses their calibration factors and the current signal readings. Solving the model's equations for the calibration factors that minimize error gives them up to date parameters for each beacon that they

then use for localizing using generic trilateration. They report a reduction in the Euclidean distance between the mean of their estimates and the actual device location, by about 50% of the error of their estimates without this dynamic update.

Another attempt to work around the noise inherent to BT signal strength beyond a few meters is that of Blumrosen et al. [9]. This work is unique among the systems presented in this thesis document, as they do not present a system for localization on the scale of within a room or within a building. They present a system that uses trilateration to localize devices to scales on the order of a tabletop, or under a half a meter. To do this, the only significant difference in their trilateration technique from other techniques, is the placement of BT beacons less than 30 cm apart, and use calibration data that maps signal strength changes to distances that are also approximately 30 cm. They report no dramatic differences in the minimum and maximum reported RSSI at the largest extent of their scale. Such work is promising for applications with positions that vary at that scale, such as localizing medical equipment during an operation. However, Blumrosen et al. do not separate the effects of small calibration distance and also placing BT beacons 30 cm apart. It is unclear whether their accuracy gains are from calibrating at a smaller distance, or from having more proximal beacons.

In summary, trilateration improves on the resolution of fingerprinting when used with BT devices as beacons in the environment. On the other hand, although BT signal strength's attenuation over distances provides an effective means of approximating distance for trilateration, its inherent noise is a major source of error in any BT trilateration system. The major challenge to improving the accuracy of BT localization using trilateration then is to compensate for erroneous signal strength readings that would imply different distances between localizing device and beacon than are the actual distances in the environment.

2.3 Alternatives

The most common BT localization systems fall into the two categories of fingerprinting or trilateration. However, localization is much more widely studied than only the case of indoor BT localization, and is applied in a variety of areas. The fields of robotics and sensor

networks in particular have their own treatments of localization. As well, trilateration is merely a subset of similar localization methods that are possible.

An alternative to trilateration is triangulation. In triangulation, a similar system of equations is used, where the unknowns in the equations are the angles of arrival of signals, instead of distances. Such systems are described in [30, 33, 34]. A problem in their implementation is that they require specialized equipment for measuring the relative angles between the localizing device and beacons. Trilateration with measures such as RSSI for estimating distances allow for generic, commercially-available BT devices to be used, with no hardware modifications. Triangulation is therefore underrepresented in the literature. However, the same general pattern exists in both strategies: first, extract information about a device's position relative to known, fixed points; then transform that information into a position based on the geometry of the situation. "Geometric localization" may perhaps be a more general descriptor; the term "trilateration" is used here because of trilateration's prevalence, and because it is the version of geometric localization performed in this thesis document.

The field of robotics views the problem of localization more broadly than BT localization does, because of the potential for a robot to be equipped with many sensors. Odometric and rangefinding sensors are common, and can be combined effectively to localize a robot in an arbitrary environment, with or without a map of the obstacles that the robot would encounter [49]. The problem of localization can then be abstracted from the question of how position estimates are achieved; often, "Simultaneous Localization and Mapping," or "SLAM," is used to refer alternately to the solutions to and the problem of localization and mapping, regardless of the sensor information used. A popular solution for this and other classes of temporal tracking is a family of techniques that are based on Markov chains, a class of Bayesian network. To represent tracking using a Bayesian network, a smaller network that represents localization at one time is repeated within a larger network. Each smaller network has variables for the positions X_i at times t_i for all times $t_i \in \{t_0, t_1, ..., T\}$ where T is the length of time being observed. The smaller networks at each time t_i form a chain, because each one is connected to the state variable nodes at time t_{i+1}. The family of techniques often use a process known as "filtering," where the network's state variables X_T at time T are queried for using an automated inference algorithm, based on observations O_i for all times

$t_i \in \{t_0, t_1, ..., T-1\}$:

$$\mathrm{P}(X_T \mid O_1, \ldots, O_T). \tag{2.6}$$

More of the specifics of Bayesian inference are described in §3.1; see Chen [10] and Fox et al. [18] for a more in depth description of filtering in specific. Without adding details now, this set of techniques requires the probability distribution $\mathrm{P}(O \mid X)$, called the observation model, describing what observations are likely to occur in a specific position. However, most localization systems that use these techniques fall into one of two categories.

- Some systems directly measure sensor information about the localizing device's position, such as distances taken with sonar or laser rangefinders [19, 49]. These measures result in observation models that equate measures to specific locations in the environment: given a position X, observations O result with probability $\mathrm{P}(O \mid X)$ [8, 19, 21, 25, 43, 44, 42, 49, 52]. This style of applying Markov chains parallels the technique of fingerprinting, where sensor information is gathered at every localizable position in the environment.

- Other systems use localization methods such as GPS or WLAN trilateration to determine a position estimate to be used as a noisy observation of the device's true position [38, 46, 50]. The Markov chain then does not represent the process of localization at all, and models only the tracking of the localizing device through time.

For example, in [49], Thrun et al. dissect the problem of localization into: position tracking, where the initial position of the robot is known concretely, but none of its subsequent positions; the global localization problem, where the initial position isn't known; and the kidnapped robot problem, where the robot changes position abruptly within the span of time for which the robot's location is desired. These divisions ignore the issue of what type of sensor data the robot is expected to use to localize itself. Thrun et al. then proceed to describe a localization system where a robot uses laser rangefinder data to localize itself: its $\mathrm{P}(O \mid X)$ is a calculated using collection of distance estimates that were measured throughout the localization space. In this sense, Thrun et al.'s work in [49] is closer to fingerprinting than to trilateration, which is undertaken in this thesis document. None of the known systems use probabilistic methods to perform trilateration by representing the relationship between

sensor information and distances as a distribution. In Chapter 3, I describe my model for probabilistically modelling the trilateration calibration between BT signal strengths and distances.

The field of sensor network localization also has its own approach to the localization problem. In the case of sensor networks, rather than localizing only a single device or robot, the location of all of the sensors is unknown: the goal is not to provide positional information to a mobile device so that the services rendered to it can be more relevant, but instead to associate the data measured by the sensors with the sensors' physical locations. Patwari et al. [34] refer to a common technique as "cooperative localization." In cooperative localization, rather than determining the location of each sensor in the network relative to a set of fixed locations, the sensors can determine their distances relative to the sensors closest to them. The knowledge of position of each of the sensors in the network can then be determined by association, provided that some devices are within range of beacons that act as "anchors" to fix the network in the real world. Multidimensional scaling (MDS) is a popular algorithm used in the field [31, 47]; the specifics of it and of the other algorithms used in the sensor networks field to abstractly incorporate the distance information provided by the sensors, are also not discussed here.

Chapter 3

Description of the Bayesian Model

Chapter 2 reported a variety of attempts to improve localization accuracy, by working around the difficulties of calibrating RSSI measurements versus the distance between two BT devices. However, none of these methods satisfactorily solved the problem. Wireless signal propagation is inherently noisy so that for a given distance, a range of possible signal strength readings exist. Multipath errors are one common cause of different signal strengths being measured between two stationary devices. If two devices are 5m apart, the measured strength of a wave that travels directly between them will be stronger than if the devices are further apart, because the signal strength is attenuated more the further that the wave travels. However, there is the possibility that the signal would be reflected off of nearby objects or obstacles such as walls: because the wave did not travel in a straight line between the two devices, the signal would necessarily have been attenuated more. For one distance, then, there could actually be a number of possible signal strengths; conversely, reading one signal strength cannot be directly mapped to a single distance. Sensor noise will therefore always be a significant source of error in any BT localization system with fixed calibration parameters.

An alternative to a closed-form calibration equation is a probabilistic model that can incorporate sensor noise of this kind. A Bayesian network is a classic tool for automated inference from the field of Artificial Intelligence [35], that can be used to describe the relationships between variables in terms of probability distributions. Once the model is built, algorithms exist for automatically combining the prior distributions that describe the variables' relationships, to answer an arbitrary query in the form of a probability statement over those variables [29, 41]. For BT localization, one can avoid fixed calibration parameters by using Bayesian networks to describe how the distance between two BT devices causes signal

strength readings to occur with specific probabilities. Localization then becomes a query of the joint distribution of the variables that represent the localizing device's position. The rest of this chapter describes the fundamentals of Bayesian networks, as well as the specific localization-modelling network that is the subject of this thesis.

3.1 Bayesian Networks

Bayesian networks are graph-based models of probabilistic relationships. In such a graph, the nodes represent the variables of the model. The nodes can represent either continuous or discrete variables; although in the model presented here, variables are discrete. The nodes are connected together with directed edges if one variable directly influences another. In most cases, the relationship between the variable at the edge's origin and the variable at the edge's end point is believed by the model designers to be causal. The networks are restricted to be directed, acyclic graphs (DAGs): if variable A causes a change to B, which in turn causes changes to C, then C is restricted from causing changes to A. With this structure as a model for any system, there are established algorithms for determining a probability distribution for a set of query variables $\{Q_1, Q_2, ..., Q_n\}$, given the knowledge that another set of variables $\{E_1, E_2, ..., E_m\}$ are in evidence with known values $\{e_1, e_2, ..., e_m\}$. All such joint probability statements will be of the form

$$\mathrm{P}(Q_1, Q_2, ..., Q_n \mid E_1 = e_1, E_2 = e_2, ..., E_m = e_m). \tag{3.1}$$

The probabilistic relationships between nodes are described by conditional probability tables (CPTs). Each variable has its own CPT that describes the conditional probability of its values given the values of nodes connected to it in the network. For a discrete variable P with no parent nodes, the CPT of P is a one-dimensional table containing the probability of each possible value of P; in the continuous case, the relationship is described as a probability density function. For a variable C that has parent nodes $\{P_1, ..., P_n\}$, the CPT of C has an additional dimension for every parent variable, because the probabilities of the values of C are now described conditionally based on the possible values of parents $\{P_1, ..., P_n\}$. As an example, if C has three parent nodes ($n = 3$), then the CPT of C is four-dimensional, and,

for all c in the set of values of C and all p_1, p_2, and p_3 in the set of values for P_1, P_2, and P_3 respectively, the probabilities listed in the CPT of C are

$$\mathrm{P}(C = c \mid P_1 = p_1, P_2 = p_2, P_3 = p_3). \tag{3.2}$$

A benefit of the graphical nature of Bayesian networks is that they allow one to infer conditional independence between variables, a process that would otherwise require algebraic effort. Conditional independence between sets of variables can be determined by a feature of DAGs called "d-separation:"

Definition 3.1 *"If X, Y, and Z are three disjoint subsets of nodes in a DAG D, then Z is said to* d-separate *X from Y, denoted $\langle X \mid Z \mid Y \rangle_D$, if along every [undirected] path between a node in X and a node in Y there is a node w satisfying one of the following two conditions: (1) w has converging arrows and none of w or its descendants are in Z, or (2) w does not have converging arrows and w is in Z." [35]*

Given this definition of d-separation, variables X are conditionally independent of variables Y given variables Z (that is, if all variables in Z are in evidence), if Z d-separates X from Y. The effect of d-separation on conditional independence can also be understood in terms of "information flow." The knowledge contained in variables that are in evidence can be said to "flow" from the evidence variables to the query variables for which a joint probability distribution is desired; the flow of knowledge is "blocked" between variables that are d-separated, causing the variables to be conditionally independent. When this concept of knowledge flow follows the definition of d-separation, it mirrors the same conditional independence that would be demonstrated by pure algebra.

Figure 3.1 presents an example network with a head-to-head node. A head-to-head node is a node where an undirected path through the node arrives at it by following an edge directed at the node, and then leaves the node by following an edge that is also directed at the node. Node C in Figure 3.1 is therefore a head-to-head node. In a network with no nodes in evidence (with no nodes in Z), the only kind of node that can block the flow of information from one node to another node and cause the two nodes to be conditionally independent is a head-to-head node. Therefore, because the undirected path from node A to node B travels through head-to-head node C, the nodes A and B are conditionally independent only if C is

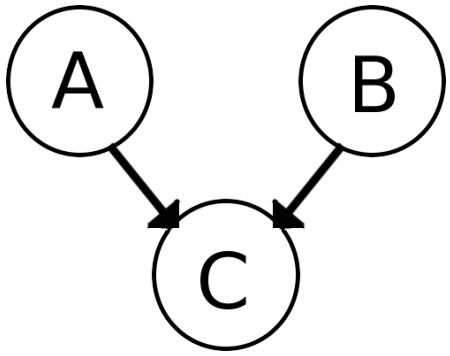

Figure 3.1: A simple Bayesian network. The node C is head-to-head for an undirected path from A to B, because the path enters C by traveling through an edge that is directed toward C and leaves C by traveling through an edge that is directed away from C. This means that node C "blocks" the flow of information from A to B if C is not in evidence; it allows the flow of information if it is in evidence. This also means that the variable A is conditionally dependent on B given C.

not in evidence. This is the first case in definition 3.1, where the variable w has converging arrows. Alternatively, C would cause A and B to be conditionally independent if one of the edges of C were reverse, and if C *is* in evidence. This is the second case in definition 3.1, where the variable w does not have converging arrows. For A and B to be conditionally dependent, either a value for C would have to be entered in evidence, or one of the edges in the network would have to be reversed to make C be not head-to-head [41]. In this way, Bayesian networks are a representation of probability models, and not a modification of standard probability laws in an effort to simplify the laws for application.

Any probability query over the set $\{P_1, ..., P_n\} \cup \{C\}$ is expressible as combinations of the probability statements associated with the network's CPTs, after the repeated application of the chain rule and Bayes' rule for probabilities. This is because the joint distribution over all the variables in the network can be factorized into the expressions for the CPTs using the chain rule for probabilities. The joint distribution of a set of variables A, B, and C, where C is a head-to-head node with parents A and B, is

$$\mathrm{P}(C, A, B) = \mathrm{P}(C \mid A, B) \times \mathrm{P}(A \mid B) \times \mathrm{P}(B) \tag{3.3}$$

by the chain rule [41], or

$$\mathrm{P}(C, A, B) = \mathrm{P}(C \mid A, B) \times \mathrm{P}(A) \times \mathrm{P}(B) \tag{3.4}$$

because of the conditional independence of A from B, based on the structure of the network. Each term on the right hand side of equation 3.4 is the probability distribution associated with a CPT of the network in Figure 3.1. Similarly, queries over subsets of the variables and over larger Bayesian networks are all representable as combinations of the CPTs of nodes in the network, because of their relationship with the factorization of the joint distribution.

Pearl's original message passing algorithm is a classic algorithm in the field, that takes advantage of the structure of the network to manipulate the CPTs into any query statement. It can be used as an example to describe the basics of the algorithmic processing of CPTs. In it, a node collects the influences from its neighbouring nodes, uses them to update its own posterior distribution, and then passes its distribution as a "message" to its neighbours, for them to repeat the process. The passing of influence messages is thus the same as the "flow" of information described earlier. The algorithm can be optimized based on the conditional independence implications of nodes in evidence and head-to-head nodes. Everywhere that information would be blocked by a node in evidence or a head-to-head node that is not in evidence, messages from earlier nodes in a path can be stopped, such that later influences would no longer incorporate the messages of conditionally independent variables [35].

Pearl's algorithm is only valid for a class of networks called polytrees, with only one undirected path through the network between any two nodes. An algorithm without this restriction is join tree propagation, which modifies the network from its original DAG to a "join tree," by converting all edges to undirected ones and adding edges between every node's parents to produce an undirected cyclic graph where cliques are families in the original network. The join tree is then produced by joining cliques together into nodes of an undirected acyclic graph: every join tree node represents a clique of nodes from the Bayesian network; a Bayesian network node appears in the join tree node for every clique it is in; in at least one join tree node, a Bayesian network node has every member of its family in the same join tree node. A similar process of influence passing is then performed using messages between the join tree nodes, based on combinations of the CPTs of the network nodes represented by each join tree node [29]. This algorithm is used in Netica, the software tool used to implement the localization models in this thesis.

It is important to note the effect that the sizes of the parent variables (in terms of the

number of values) have on the size of the CPT (in terms of the number of probabilities to store). Because each node's CPT contains the probability of every value of that node given all the possible combinations of the parents' values, the size of the CPTs grow as the product of the sizes of the variable and the sizes of all its parents. For a family of nodes containing the child node C with size $|C|$ and parents $P_i \in \{P_1, ..., P_p\}$ with sizes $\{|P_1|, ..., |P_p|\}$, the size of the CPT of C is

$$|C| * \prod_{i=1}^{p} |P_i| \tag{3.5}$$

Representing larger CPTs in an implementation incurs memory costs; iterating over larger CPTs in algorithms incurs computational costs.

The relationship between CPT size and computational cost can be explained in terms of the structure of the join tree. In building a join tree, there is often more than one way to group network nodes into join tree nodes.[1] The width of a join tree is the size of the largest node in that tree, in terms of the number of Bayesian network nodes represented in it. The induced width of a Bayesian network is the smallest possible width among the possible join trees. The space and time complexity of Bayesian network inference is exponential in the induced width of the network [13]. If the family $\{P_1, ..., P_p\} \cup \{C\}$ is the largest family in the Bayesian network in terms of the number of nodes in the set, and if it is possible to build a join tree such that that family is the largest node in the join tree, then the induced width is $1 + p$. Although it is possible for the induced width to be larger than the largest family, the largest family is a lower bound on the possible induced width of a Bayesian network. Adding edges such that the largest family has more variables in it, and adding values to the variables in the largest family, will both increase the computational requirements of using a Bayesian network.

[1] One of the steps to constructing a join tree, before combining Bayesian network nodes into join tree nodes consisting of families, is to triangulate an undirected graph of Bayesian network nodes until it is chordal. A chordal graph has no undirected cycles of four nodes or greater that do not have a chord connecting two non-adjacent nodes in the cycle. In the process of triangulating the undirected graph, the choice of which to nodes to join by an edge is irrelevant to the legitimacy of the subsequent join tree. However, the join tree nodes are each made up of the nodes in the maximal cliques of the triangulated graph, and so the choice of chordal edge to add can change the structure of the resulting join tree.

3.2 Discrete Representation of Location

To model BT localization using Bayesian networks, one first has to develop a model of the space within which the BT devices will exist. In my model, I represent two-dimensional location with two Bayesian network nodes, one for each spatial dimension. Because each of these variables is discrete, I necessarily divide each spatial dimension into a finite number of values. A position within space then is a combination of specific evidence values for each of the nodes. Mathematically, for variables X and Y, with values $\{x_1, x_2, \ldots, x_{|X|}\}$ and values $\{y_1, y_2, \ldots, y_{|Y|}\}$ where $|X|$ and $|Y|$ are the number of values of both variables, their CPTs express $\mathrm{P}(X)$ and $\mathrm{P}(Y)$, because there are no parent variables that cause location. In my model, because there is no prior information as to where a localizing device or beacon would be, I set the CPTs for each variable to be uniform. All entries in the arrays representing the CPTs of all of the positional nodes, for the localizing device and beacons alike, are therefore identical floating point values, equal to $\frac{1}{|X|}$ and $\frac{1}{|Y|}$ after normalization.

For each BT device present in the system, I can replicate this representation of space. Each device's position can then either be queried for, or be entered in evidence. For a BT localization system in specific, query for the position of the localizing device given the position of every beacon as evidence. Barring the evidence of sensor readings (described in §3.5), for a system with n beacons the localization query is thus of the form

$$\mathrm{P}(X^l, Y^l \mid X^{b_1} = x^{b_1}, Y^{b_1} = y^{b_1}, \ldots, X^{b_n} = x^{b_n}, Y^{b_n} = y^{b_n}), \tag{3.6}$$

where the superscript l denotes variables of the localizing device, and the superscript b_i denotes variables and possible values of the i-th beacon.

3.3 Discrete Representation of Distance

I represent the distances between a localizing device and each of the beacons with new distance nodes, each with incoming edges from the position nodes of the localizing device and from the position nodes of one associated beacon. The distance nodes are also discrete, such that there are a fixed number of possible values, representing ranges of exact distances. The

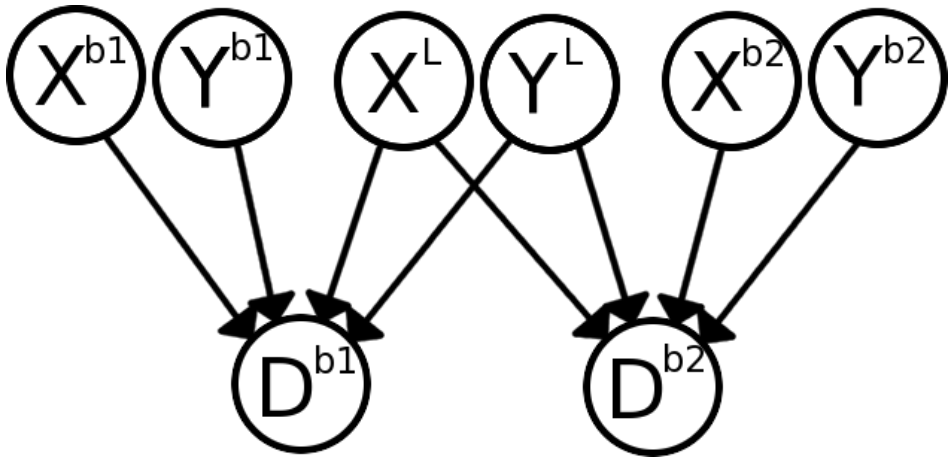

Figure 3.2: A Bayesian network that relates the position of a localizing device with the positions of two beacons. The position nodes of the localizing device are, X^l and Y^l; the positions of the two beacons are X^{b_1} and Y^{b_1}, and X^{b_2} and Y^{b_2}. They are related through the distances between them, represented by the nodesD^{b_1} and D^{b_2}.

distance nodes act as explanatory children variables with values that depend on parent position values, so that information can flow from observations of the beacon position variables to the localizing position variables. Figure 3.2 gives an example network with two beacons and one localizing device, and the associated distance nodes that connect them.

For a distance node in my model, the CPT of that node is a five-dimensional array: one dimension for each of the parent position nodes, plus one dimension for the distance node. Given two fixed points in space labelled $\langle x^l, y^l \rangle$ and $\langle x^b, y^b \rangle$, the Euclidean distance between those two points is fixed. For all combinations of distance values $d_s^b \in \{d_1^b, \ldots, d_{|D|}^b\}$, values x^l and y^l of the localizing device's two position nodes, and values x^b and y^b of one beacon's two position nodes, the CPT contains the probabilities

$$\mathrm{P}(D^b = d_s^b \mid X^l = x^l, Y^l = y^l, X^b = x^b, Y^b = y^b). \tag{3.7}$$

This representation of distance is a deterministic relationship expressed with probabilities: my representation discretizes the possible Euclidean distances, and assigns a probability of 1 to the correct distance value given two positions. Whether the distance between the BT devices at the two given locations is within the range represented by the value $D^b = d_s^b$, is

therefore either true or false:

$$\mathrm{P}(D^b = d_s^b \mid X^l = x^l, Y^l = y^l, X^b = x^b, Y^b = y^b) \\ = \begin{cases} 1: & d_{s-1}^b < \sqrt{(x^l - x^b)^2 + (y^l - y^b)^2} \leq d_s^b \\ 0: & \text{otherwise} \end{cases} \tag{3.8}$$

However, one can use a Bayesian network inference algorithm to invert this probability expression, and respond to any arbitrary query over the variables in the net. For example, I could set in evidence the position of one BT beacon, and set in evidence a specific distance, and query the Bayesian network for the joint distribution of the position nodes of the localizing device:

$$\mathrm{P}(X^l, Y^l \mid D^b = d, X^b = x^b, Y^b = y^b) \tag{3.9}$$

This is a two dimensional distribution, with a ring of higher probability around the point $\langle x^b, y^b \rangle$ specified as the location of the beacon: the inner and outer radii of the ring would be equivalent to the minimum and maximum of the range of distances represented by the chosen value for the distance node. Figure 3.3 demonstrates a distribution of this shape. Adding two other beacons, the query

$$\mathrm{P}(X^l, Y^l \mid D^{b_1 - b_3} = d^{b_1 - b_3}, X^{b_1 - b_3} = x^{b_1 - b_3}, Y^{b_1 - b_3} = y^{b_1 - b_3}) \tag{3.10}$$

where $Z^{b_1 - b_n} = Z^{b_1 - b_n}$ expands to $Z^{b_1} = z^{b_1}, \ldots, Z^{b_n} = z^{b_n}$, would produce a distribution equivalent to the single intersection of three rings that is produced in solving the system of equations for trilateration.

The position of the localizing device is conditionally independent of the positions of the beacons when the distance nodes are not set in evidence, because the distance nodes are head-to-head: without their evidence of how far apart two devices are, the evidence of where a beacon is can have no effect on the joint distribution $\mathrm{P}(X^l, Y^l)$. To implement BT localization, one has to add the relationship between distance and signal strength to influence distance, which in turn influences $\mathrm{P}(X^l, Y^l)$. One can add a node representing RSSI, with a specific beacon's distance node as its parent. The RSSI nodes would have potential RSSIs as values, to be set in evidence from observed data from the associated beacon. The CPT of each RSSI node would then represent the probability of observing a signal strength given a

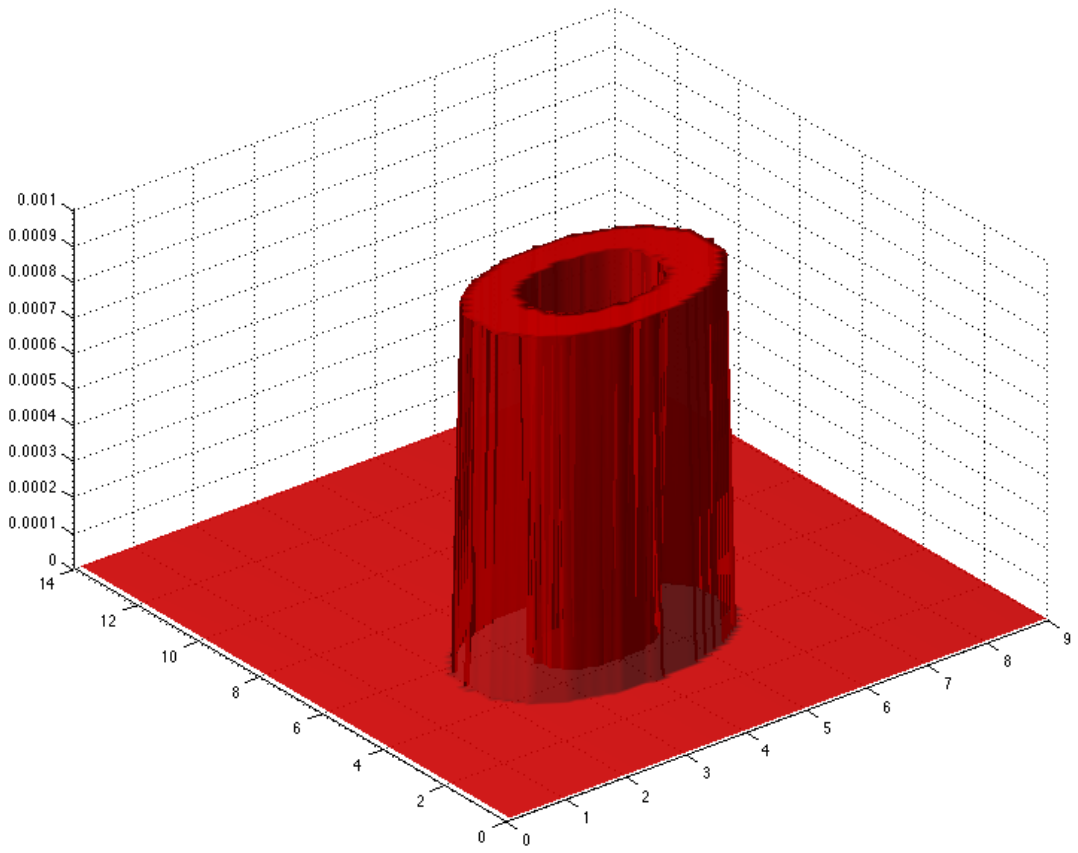

Figure 3.3: A three-dimensional plot of the two-dimensional probability distribution for the position of a localizing device known to be between 1m and 2m of a beacon's fixed position at $\langle 5, 4 \rangle$, with uniform likelihood. The size of the space was chosen to be 14m by 9m to match the space used in my experiments in Chapter 4. The distribution uses bins that are combinations of discrete spatial values; the bins are each 0.01m^2 in area. The normalized probability of a bin in the ring-shaped plateau is 0.0011.

specific distance. Similar to eq. 3.9, the query for the localizing device's position distribution would be

$$\mathrm{P}(X^l, Y^l \mid S^b = s, X^b = x, Y^b = y). \tag{3.11}$$

In eq. 3.9, the evidence for D^b influenced the distribution of positions for X^l and Y^l. With signal strength node S^b set in evidence with value s but D^b not set in evidence, the posterior distribution of D^b is influenced by S^b and in turn influences the distribution of X^l and Y^l. The difference is that there would no longer be a known distance between the beacons and the localizing device, but rather a distribution of possible distances. The resulting localization solution would be less specific than with a non-probabilistic calibration, but would incorporate the inherent noisiness of the signal reading

Recall that the CPTs of any node grow as the product of the size of itself and of all of its parents. The size of the distance nodes' CPTs are $|X|^2 * |Y|^2 * |D|$. The distance nodes' CPTs, because of this growth relationship and the characteristics of the space used in experimentation in Chapter 4, play the largest role in the breadth of the experiments that can be performed.

3.4 Discrete Representation of Pairs of Angles

Signal strength in general depends not only on the distance of signal transmission, but also on the physical properties of the transmitter and receiver. Normally, the physical features of the BT devices are not explicitly accounted for in a BT localization system, because of the added time it takes to gather appropriate data, because of the complexity it adds to a system, and the loss of generality due to algorithms that are traditionally written specifically for a given set of transmitters and receivers. The features of the transmitters and receivers are implicitly included, however, in the calibration. When a distribution of RSSIs is recorded between two devices at a specific distance, part of the spread of that distribution is caused by the physical features of the device: the impedance of the case around the device, natural signal emissions of other electronics in the device, and any number of other possible effects can all interfere with signal propagation. But in the same way that distance can be controlled for in calibration, so can some other aspects of two devices' signal interactions. In particular,

Figure 3.4: An Apple iMac, with a circle around the approximate location of the BT antenna in the model of iMacs used in this thesis.

I chose to calibrate based on the combination of distance and device orientation.

When measuring the BT signal strength between two iMacs at a fixed distance, the RSSI varies with relative orientation. In the generation of iMacs used, the BT antenna is in the upper right side as a person faces the screen, as shown in Figure 3.4. When the iMacs were oriented relative to each other such that their antennae were closer to the other iMac, the RSSI increased. I also found that the iMacs' glass screens had higher impedance to BT microwaves than their plastic backs: when two iMacs were oriented such that their screens were facing each other, they displayed a decrease in the mean observed RSSI by distance compared to when they had their backs to each other, even though the effective distance between their BT antennae was the same.

Bahl and Padmanabhan [5] and Cheung et al. [11] both measured the effects of orientation for devices other than iMacs. Though they both found that orientation could affect signal propagation, neither included orientation modelling in their implemented systems. As well, although angle of arrival information is used among some systems to perform triangulation, no published trilateration systems have described an orientation-sensitive calibration.

To model BT's sensitivity to orientation, I added an orientation node as an additional dimension to the network representation of a device's pose. The discrete values of these nodes represent a global orientation relative to the environment. The values are ranges of angles centred about 0°, 90°, 180°, and 270°, where an orientation of 0° with respect to the

environment means that the iMac's screen is facing what was chosen as the positive X axis for the environment. However, I made these angles represent global orientation rather than the relative angle between devices in the same way that the spatial representation is not relative to other devices, so that beacons' positions and orientations can be set relative to the external world I localize with respect to.

However, iMacs' *relative* orientations affect signal strength, not their global orientations. To translate from the devices' global orientations to their relative orientations, I added another variable, with parents that are the position and orientation nodes of the localizing device and a beacon. These nodes represent the model of impedance between two iMacs at relative orientations. The node has 16 values, that are every combination of two angles. The node is another deterministic node akin to the distance nodes, in that, given values for its parent nodes (four position nodes and two orientation nodes), there is one possible relative orientation of localizing device towards beaconing device and vice versa. The size of the impedance model nodes is $|X|^2 * |Y|^2 * |T|^2 * |I|$, where T nodes are the orientation nodes, and I nodes are the impedance nodes.

For example, if two iMacs have global orientations of 0° by facing the positive X-axis, and the localizing iMac is to the left of the beaconing iMac, then it is certain that the beaconing iMac has its BT antenna pointing towards the localizing iMac, whereas the localizing iMac has its BT antenna further away from the beaconing iMac. This situation is depicted in Figure 3.5. There is no other possible relative orientation for iMacs; that combination of angles' probability is set to 1 in the node's CPT, and all other combinations of angles' probabilities, given those parent values, are set to 0. For another system of BT devices with a different structure, a similar Bayesian network could be devised.

3.5 Signal Strength given both Distance and Orientation

In §3.3, I described a straightforward method of modifying a distance node such that it could be influenced by a signal strength reading and in turn influence the joint distribution of the localizing device's position. This description was accurate for a model that includes only

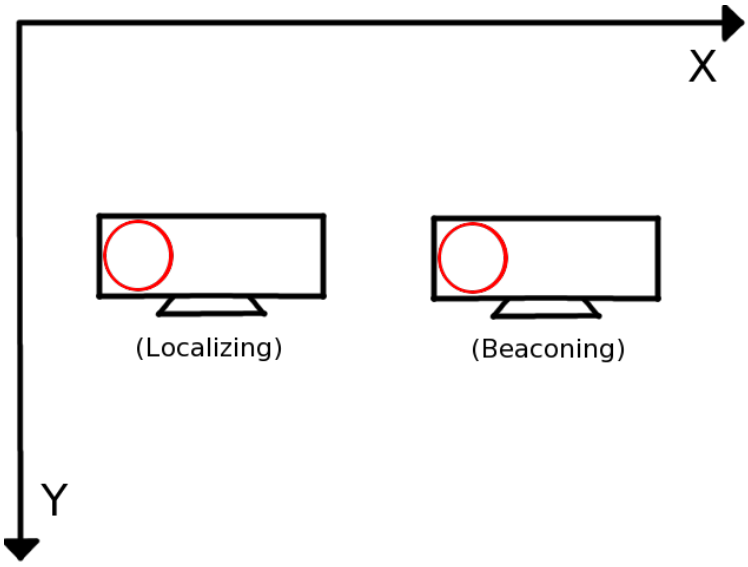

Figure 3.5: An example pair of iMacs to demonstrate the difference between their global and relative orientations. Both devices have global orientations of 0° because they are facing the positive X-axis. However, their combined relative orientation is based on how the beacon, to the right, has its BT antenna closer to the localizing device than its centre, and how the localizing device, to the left, has its BT antenna further from the beacon than its centre.

positions, distances, and signal strength readings. To add orientation is just as straightforward: the signal strength node that originally had only a distance node as a parent gains an impedance node as a parent, as both distance and impedance model can influence the signal strength observed. The signal strength node's CPT now reflects the probability of seeing a specific RSSI, given a distance and a relative orientation of two iMacs. The CPT is equivalent to the distance versus signal strength calibration of a non-probabilistic trilateration scheme as described in §2.2, except with the added information of BT device orientation.

3.5.1 Calibration Procedure

As with all Bayesian network nodes, the signal strength nodes' CPTs present the probability of a signal strength reading, given the parents' distance and impedance model. The method for filling the CPTs of the signal strength node with likelihoods drawn from real data, is similar to the calibration process for generic trilateration. If one were calibrating for generic trilateration, one would gather signal strength readings at a variety of distances; for

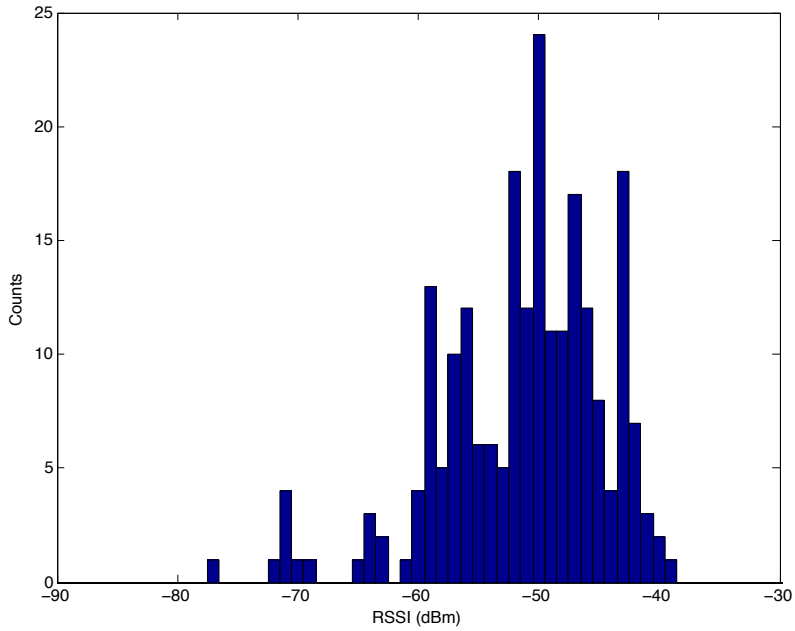

Figure 3.6: A histogram of the signal strengths gathered for calibration, given a 2 m distance between two iMacs. The histogram is a combination of the calibration data for all 16 relative orientations. The signal strength readings roughly follow the shape of a log-normal distribution, as is typical for signal strengths at a fixed distance.

probabilistic calibration, one has to gather distributions of signal strength readings at every distance and every orientation combination used in the model.

To gather this data, two iMacs were placed on top of wheeled carts, both a meter high, so that the iMacs were at constant, equal heights, and could be moved to various distances apart. One iMac was set to record signal strengths from every BT device that was within range and discoverable, and the other iMac was set to be discoverable. Then, with the iMacs and their carts at distances of 2 m, 4 m, 8 m, and 12 m, the recording iMac was set to each of the four orientations; and for each of the recording iMacs' four orientations, the transmitting iMac was set to each of the four orientations. For each of configuration of two iMacs' four orientations, the iMacs were allowed to broadcast BT discoverability and measure RSSIs from all discoverable devices in range, for five minutes. This gave approximately 14 signal strength readings for every combination of parent node values. Figure 3.6 contains a histogram of the signal strength readings measured at 2m and all relative orientation combinations.

These RSSIs were then used as samples from the natural distribution of RSSIs for a given distance and orientation combination. To interpolate a distribution for all possible RSSI from

these samples, their mean and standard deviation were used as parameters to a log-normal curve of the form

$$\mathrm{P}(S^b = s \mid D^b = d, I^b = i) = \frac{1}{s\sigma_{d,i}\sqrt{2\pi}} \exp\left(-\frac{(\ln s - \mu_{d,i})^2}{2\sigma_{d,i}^2}\right) \tag{3.12}$$

where $\mu_{d,i}$ and $\sigma_{d,i}$ are the mean and standard deviation of the logarithms of the signal strengths collected for the combination of values of distance and impedance d and i. The values s used for S were the RSSIs from -30dBm to -90dBm. These discrete distributions were then normalized, and used as the CPT for RSSI given distance and orientation.

Some of the RSSIs were removed from the calibration data if their values were outside of a standard deviation from the mean of the data. Before cleaning, the histograms of 42 calibration datasets did not match the shape of a log-normal distribution typical of signal strengths at a fixed distance: their maximum was not at the leading edge of the curve, and the lower values than their maximum would occur almost as often as the maximum rather than trailing off. I believe this was likely due to sampling error caused by the noisiness of signal strength readings, which was made prominent by our small sample size. To reduce the effect of extreme outliers on the curve calculated by equation 3.12, individual readings of low RSSI were removed with the goal of reshaping the curve such that the mean and max of the distribution were closer together; and also reshaping the curve such that the tail of the distribution was neither too large nor absent. To this end, occasionally, a single reading would be removed such that an RSSI value would no longer occur in a data set; and occasionally, two or three readings at one RSSI value would be removed, leaving behind enough readings at that RSSI value that the mean approached the max without narrowing the distribution to too few RSSI values. For example, in the case where two iMacs were 2 m apart, with the iMacs at relative angles of 270° and 90°, half of the signal strengths were removed. In this case, cleaning resulted in six remaining signal strength values, the fewest among the cleaned calibration data sets. Figure 3.7c contains histograms of the calibration data for this combination of values, before and after the cleaning process; Figures 3.7a and 3.7b contain other examples, with parameter value combinations of 2m, 180°, and 90°, and 12m, 0°, and 180°, respectively. After cleaning the calibration data, the mean number of recordings per data set among the 42 cleaned data sets was decreased to 10.52 from the

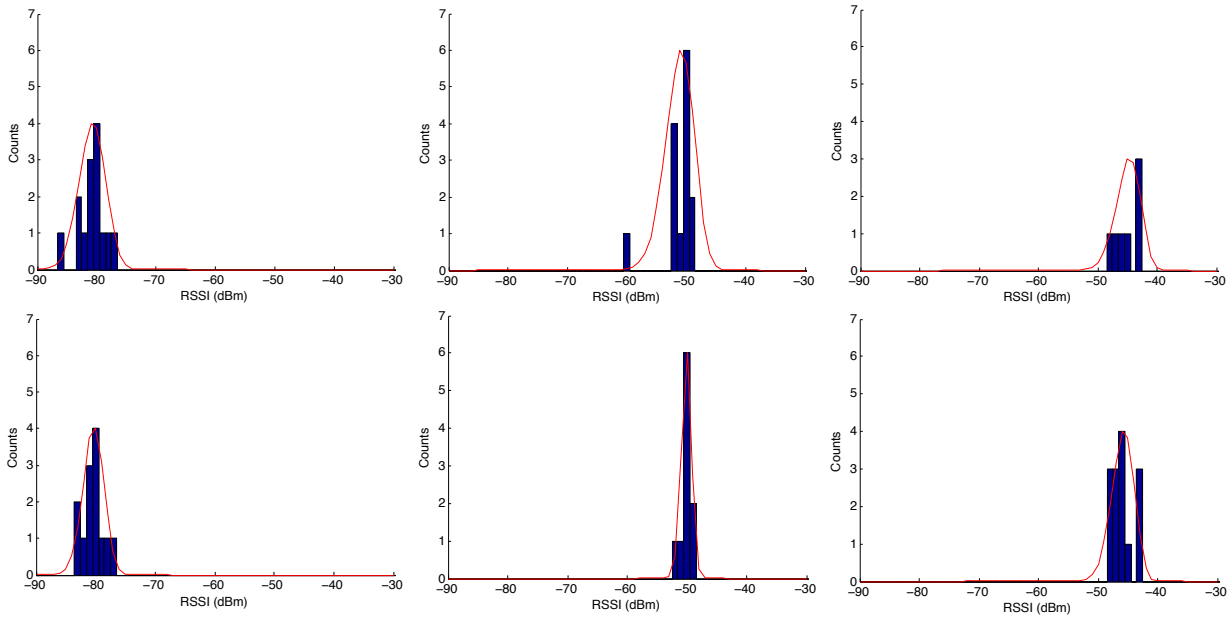

(a) One data point removed. **(b)** Three data points removed. **(c)** Seven data points removed.

Figure 3.7: Histograms of the calibration data used for distance and impedance model values. Above is the data before cleaning; below is after cleaning.

original mean number of recordings of 14.

Figure 3.8 contains distributions that were calculated in this way, where d is set to 2 m and the angle of one iMac is fixed such that its antenna is pointed towards the other. There are four subfigures, 3.8a–3.8d, that present the distributions in the CPT that follow the rotation of one iMac through four 90° increments. The subfigures are captioned with global orientations that the localizing iMac in Figure 3.5 would have as it rotates, while the beaconing iMac remains fixed with its antenna towards the localizing one. The distributions start with the rotating iMac's antenna towards the fixed iMac, with the highest mean RSSI. The distributions continue through two clockwise increments of 90° as the rotating iMac's antenna moves away from the fixed iMac; their mean RSSI decreases. In the last 90° increment, the rotating iMac's antenna moves towards the fixed iMac, but the mean RSSI still decreases, because now the glass screen of the rotating iMac is facing the fixed iMac.

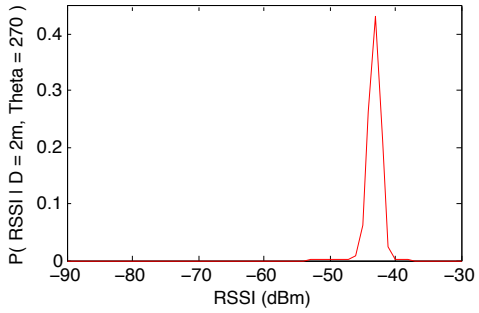

(a) 180° global orientation

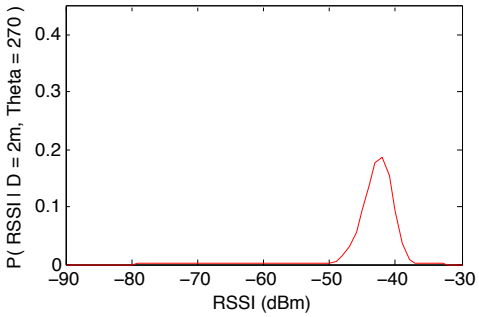

(b) 90° global orientation

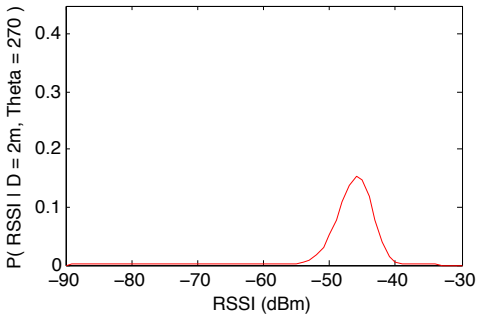

(c) 0° global orientation

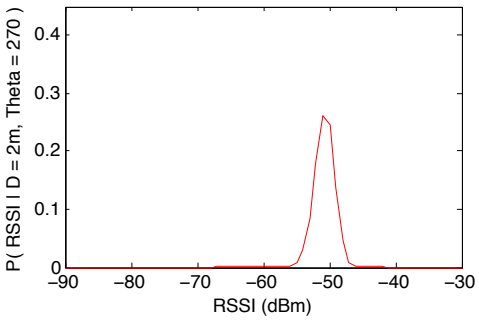

(d) 270° global orientation

Figure 3.8: A subset of the CPT for signal nodes. The curves are $\mathrm{P}(S^b | D^b = d, I^b = i)$ where $d = 2$ m, and i is varied by fixing one iMac with its antenna towards a second, rotating iMac. Subfigure 3.8a is calculated from data gathered when the iMacs are oriented with their antennae towards each other; the rotating iMac's antenna is moving away from the other iMac in subfigures 3.8b–3.8c; and in subfigure 3.8d, the rotating iMac's antenna has moved closer to the fixed iMac, but the rotating iMac's glass screen impedes signal propagation.

Chapter 4

Experimentation

In Chapter 3, I introduced a Bayesian network designed for localizing a BT device using other BT devices as beacons in a trilateration system, with a probabilistic calibration of the decrease in signal strength in proportion to the distance between BT devices. As mentioned, the size of the variables will drastically affect the space and time requirements of computation. For this reason, many practical applications of such systems will perform a number of optimizations to compile a Bayesian network from an abstract structure capable of responding to any query, into a form that can only answer the single intended query of device localization. However, I can use a generic Bayesian network built with discrete variables to experiment with the effects of varying a number of parameters that are not present in either a continuous Bayesian network, or a non-probabilistic model. For example, because the distance and orientation nodes each have four position nodes as parents, if the number of position values doubles by decreasing the size of the discrete bins that divide the localization environment, the space required for the distance and orientation CPTs will increase by a factor of 2^4. Modifications of this magnitude therefore quickly become intractable in a production system. By making adjustments of this scale in an offline situation, though, I can do so repeatedly in spite of computation time, to explore how accuracy is affected as such parameters are varied. In §4.3, I present the results of using 2.0 m, 1.0 m, 0.5 m, and 0.2 m as the size of discrete position bins. Each of these scales increases the memory requirements and computation time of Bayesian inference by roughly a factor of 2^4 when compared with the next larger scale.

Another parameter I vary is the number of distance values used. As described in §2.2, Blumrosen et al. [9] demonstrated that BT trilateration could be used to localize a device with a resolution under a meter. However, the remainder of the literature does not rigorously

perform calibration of BT signal strength versus distance below one meter. As well, as mentioned in Chapter 1, the more rapid decrease of BT signal strength with distance when compared to WLAN signal strength decrease, can potentially result in a smaller resolution to BT trilateration. To explore whether localization accuracy can increase by using distance calibration at or below 1.0 m, and by dividing the effective range of BT into more distance values, I repeatedly simulated localization using Bayesian networks where I doubled the number of distance values in the model from the default values of {2 m, 4 m, 8 m, 12 m} to {1 m, 2 m, 3 m, 4 m, 6 m, 8 m, 10 m, 12 m}. The results are presented in §4.5.1.

I also experimented with the number of beacons the model uses for localization, in §4.5.2. Non-probabilistic trilateration as it is normally implemented, described in §2.2, combines distance information from $d + 1$ beacons, where d is the number of spatial dimensions of the resulting location estimate. Among the known literature, only Fernandez et al. [15] have studied the effects of varying the number of beacons used. It is generally unknown, then, whether distance information from additional beacons can improve accuracy, or if information from fewer beacons would decrease accuracy. With no other given information, however, incorporating the signal strength readings from additional beacons should decrease the probability that one of those signal strength readings would be erroneous, and that fewer beacons should increase that same probability. In a probabilistic model of trilateration, the information from any number of beacons can be combined to produce a single location estimate by simply repeating pieces of the original Bayesian network. I therefore repeatedly simulated localization with a range of numbers of beacons, from 0 beacons to 8 beacons, to determine how the number of beacons can affect localization.

An important consideration when dealing with discrete variables is how rounding can affect the ensuing results of calculations. To determine whether rounding had an effect on the accuracy of my experiments, I undertook two other sets of repeated simulations of localization. In §4.4.1, I describe how I varied the position of the devices within spatial bins, to determine if localization is affected when probability mass that would in the continuous case occupy the exact position of a localizing device is rounded into the closest spatial bins. In §4.4.2, I vary the proximity of the devices to the edges of the represented space, to determine if localization is affected when probability mass is constrained to be within the

dimensions of the represented space when in the continuous case it might occur outside this range. §4.4 is in sum the section that presents validation results that are specific to models built using discrete variables, whereas §4.5 presents results that I believe to be generalizable to other indoor BT trilateration systems. §4.1—4.3 are dedicated to introducing my experimental methodology.

4.1 Data Collection

I collected signal strength readings between iMacs in a teaching laboratory in the Dept. of Computer Science on the campus of the University of Saskatchewan, so that I could perform the offline experiments using my model with data gathered in a realistic environment. The size of the room was 14m by 9m. The room had approximately 35 iMacs. Fifteen iMacs were chosen for the study among the 35, such that the chosen iMacs were spaced apart by at least 1.6 meters. Because of the purpose of the room as an instructional lab, the iMacs were in roughly a grid formation. The positions of the fifteen iMacs were measured relative to the stationary desks in the room, to be used as ground truth. The laboratory was left locked while the iMacs actively collected data for roughly 24 hours. All iMacs other than the chosen fifteen were turned off for the duration of the study.

The iMacs were all booted from identical Ubuntu 11.04 LiveCDs. Each iMac ran a Python script that recorded the RSSI values from every discoverable BT device within range, along with the BT MAC addresses of the corresponding devices. All of the iMacs were set in BT discoverable mode, so that every participating iMac recorded signal strengths from every other participating iMac. The RSSI values from any other discoverable BT devices were filtered out of the resulting data. The signal strength and MAC address combinations were collected on a remote server for analysis after the fact. In this way, between 6350 and 6715 RSSI readings were gathered between every pair of the fifteen participating iMacs, with an average of 6615 readings.

Not all of the 15 recording iMacs were used in my experiments, to avoid assigning inaccurate orientation values to some of the beacons. All of the iMacs in the room were oriented towards the centre front of the room, so that students at the iMacs could all face a lecturing

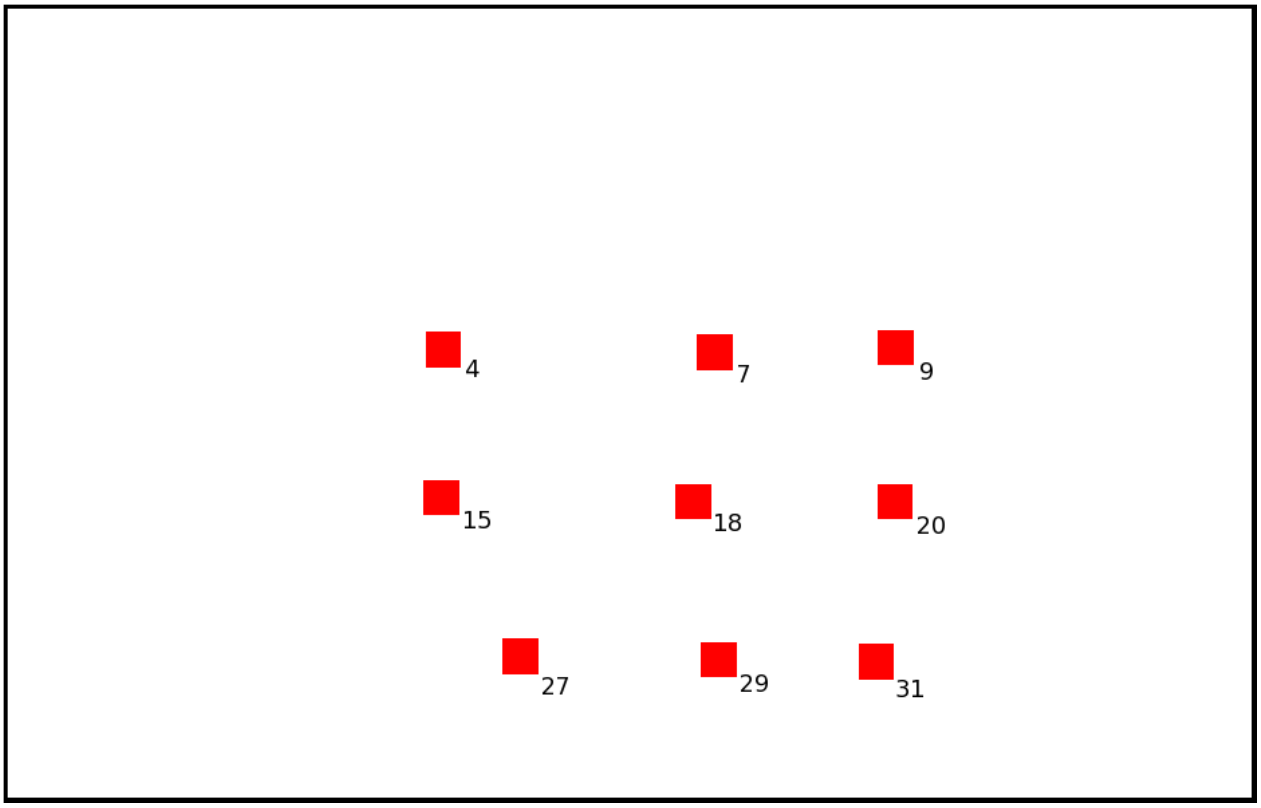

Figure 4.1: A map of the space used for gathering experimental data. The red squares are centred at the positions of the nine iMacs used in the study. The iMacs in the map are labelled with the numbers used to identify them in the lab. The width of the room is 14m; the height is 9m.

Teacher's Assistant. In the centre of the room, this meant that iMacs were all roughly rectilinear with each other, with orientation variations of much less than 45° either clockwise or counterclockwise. At the edges of the room, however, the iMacs were turned approximately 45° relative to the iMacs at the centre of the room. To use all 15 iMacs would mean that the orientation values for the iMacs at the sides of the room would be on the boundaries between two of the four possible orientation values. The orientation angles were not accurately measured at the time of data collection to be able to choose an orientation value with certainty; and doubling the number of orientation values would double calibration time and possibly double the memory requirements of the model. To avoid either the cost of inaccurate values or extra orientation values, I used only the 9 iMacs that were at the centre of the room, omitting the 6 iMacs that were along the two sides of the room. Figure 4.1 shows the positions of the chosen iMacs within the room.

4.2 Offline Simulation of Localization

Using the data gathered in §4.1, I can simulate instances of localization within the room by choosing a set of iMacs from among the central nine iMacs, choosing one iMac among them to act as a localizing device, and using the positions and signal strengths from the remaining iMacs as evidence to the model. By leaving out the position of the localizing iMac instead of entering it as evidence, I can query for the iMac's position distribution, and compare that estimated position with the iMac's actual position as a measure of accuracy. I can then explore how a parameter of the model affects localization accuracy in a hypothetical environment.

The general procedure of each experiment described in the following sections begins with building the Bayesian network according to the parameters of the current experiment. For example, a structural parameter of the model is the number of beacons, requiring a completely different instance of a Bayesian network with a different number of beacons, if that is the parameter being varied in the experiment. Given a network built to the current parameters, the positions of the iMacs currently being used as beacons are entered as evidence to the appropriate nodes. As well, a localizing device is chosen from among the set of iMacs being

used in the experiment. The position of the localizing device is not entered as evidence, as the distribution that estimates its position is the query distribution I am interested in. After the beaconing iMacs' locations are entered, signal strength readings between each beacon iMac and between the localizing iMac, taken from among those recorded in the 24 hour period, are entered as evidence.

Sample signal strengths were drawn from the recorded signal strengths. If iMac a were the localizing device, then the approximately 6000 signal strengths it recorded from beaconing iMac b were given equal weight as probable observations by iMac a from iMac b. To do this, a random integer was chosen between 1 and the number of recordings made by iMac a from iMac b; this integer was used as an index into a sorted list of the recordings, and the value at that index was used as an observation. In this way, I can simulate live signal strength readings based on real data, with the same likelihood of random noise as was actually observed in the environment. This process was repeated such that 50 trials were generated and evaluated for any single combination of experimental parameters.

The Bayesian networks used for this evaluation procedure were built using the Netica software package developed by Norsys.[1] The implementation of the model, and its evaluation, were written in Java. Various pieces of the experimentation were performed on three distinct computers, though this only affected the length of computation, based on the computers' respective speeds and amount of RAM installed. One machine used was a desktop iMac model "iMac8,1": it had a 2.4GHz Intel Core 2 Duo with 3GB of RAM installed. Another machine was a server maintained by the University of Saskatchewan Computer Science Department's ARIES lab: it had two Intel Xeon dual-core processors with hyperthreading, and 8GB of RAM. Another machine was a server maintained by the University of Saskatchewan Information and Communication Technology Division: it had four Intel Xeon Quad-core processors and 256GB of RAM.

[1] `http://www.norsys.com/netica.html`

4.2.1 Euclidean Distance from the Distribution's Maximum versus its Mean

A natural method for evaluating the accuracy of a localization system, used throughout the literature, is simply the Euclidean distance between the estimated position of the localizing device and its ground truth location. However, the Euclidean error distance is not straightforward to calculate from the results of my model. Whereas most localization techniques produce a single point which a Euclidean distance can be calculated from, probabilistic methods produce the position of the localizing device as a distribution over two dimensions. The Euclidean distance can therefore only be calculated from some summarizing measure of the resulting distribution. As no known other localization works use Bayesian networks so directly as to produce discrete probability distributions from BT readings, a reasonable evaluation method was required.

Taking the Euclidean distance from the distribution's bin with maximum value is an intuitive way of using a summarizing measure to achieve a single value for error:

$$\langle m_x, m_y \rangle = \arg\max_{x,y} \mathrm{P}(X = x, Y = y \mid \mathrm{Data}) \tag{4.1}$$

$$\mathrm{Error} = \sqrt{(m_x - \hat{x})^2 + (m_y - \hat{y})^2} \tag{4.2}$$

where $\langle \hat{x}, \hat{y} \rangle$ is the ground truth position. In an ideal case for localization, with perfect signal strength readings taken from an adequate number of beacons for trilateration, there will be a single pair of values $\langle x, y \rangle$ containing all of the distribution's probability mass, the remaining bins of the discrete distribution will have zero probability mass, and the area that the bin $\langle x, y \rangle$ represents will contain the actual position of the localizing device. Although this error measure would only be precisely zero if the localizing device were centred in the bin that contains it, measuring the Euclidean distance in this way, for this hypothetical case of minimum error, will produce the minimum possible error distance measure for that localizing device's position. In this way, this error measure's value decreases as the accuracy of the distribution's most likely estimate of position increases.

It is a desirable quality of an error measure to penalize a distribution that is accurate but that is uncertain in its estimate. For decreasing certainty of the localizing device's

position, with probability mass spread throughout the distribution instead of concentrated in one bin, error measured from the distribution's maximum does not necessarily decrease. For example, if all but the correct bin contain equal amounts of probability mass, and the correct bin contains a slight amount more probability mass, the Euclidean distance from the maximum of the distribution to the correct position is the same as in a certain case.

A method that takes into account the entire estimate distribution is to measure the Euclidean distance from the weighted mean of the distribution:

$$\mu_x = \sum_{i=0}^{|X|} i \times \mathrm{P}(X = i \mid \mathrm{Data}), \quad \mu_y = \sum_{j=0}^{|Y|} j \times \mathrm{P}(Y = j \mid \mathrm{Data}) \tag{4.3}$$

$$\mathrm{Error} = \sqrt{(\mu_x - \hat{x})^2 + (\mu_y - \hat{y})^2} \tag{4.4}$$

where $\langle \hat{x}, \hat{y} \rangle$ is the ground truth position. This allows inaccurate bins with probability masses between zero and the distribution's maximum to still affect the error distance, if enough probability mass exists in the inaccurate bins to shift the mean of the distribution away from the maximum, and possibly also from the correct position. Thus, this measure penalizes uncertain distributions.

Both methods have issues in the special case of a uniform distribution that can make them difficult to interpret. In the case of the Euclidean distance from the mean, the mean of a uniform distribution is its centre, and in my gathered data, the iMacs are clustered near the centre of the room, because of the functional demands of the laboratory for everyday use. This means that in my evaluations, uniform distributions will often produce lower error measures than expected. In the case of the Euclidean distance from the maximum, a uniform distribution has no maximum. The evaluation method, as implemented, simply chooses the first distribution bin encountered with the maximum, and the bins are iterated through in index order, starting in one corner of the room. Because, as mentioned, the iMacs used are mostly in the centre of the room, measuring error from the distribution maximum will often result in error distances that are approximately equal to the distance from the centre of the room to one of the corners — the maximum possible error distance for a device in the room's centre. Alternatively, I could adjust the size of the represented space so that it was not the same size as the room, by either shrinking the represented space or by growing it an arbitrary direction. However, if I were to shrink the size of the space from the actual size

of the room, so that the iMacs were not at the centre of the represented space, then edge effects would become apparent, as demonstrated in §4.4.2; and if I were to grow the size of the room, this would drastically increase the memory and computation requirements of my Bayesian network implementation, as has been already discussed. Therefore, I explore the effects of these two evaluation measures in §4.5.2, but continue to use the size of the original room as the size of the represented space. In general, the Euclidean distance from the mean is used for evaluation, except where otherwise specified.

4.3 General Accuracy Results

Before measuring the effects of a larger variety of parameters, I should establish whether my model can achieve a standard level of accuracy comparable to that achieved in the field, without the application of extreme parameter values for experimentation. My general results are presented in a range of values for the parameter that most directly results from using discrete variables: the scale of the spatial variables representing position. I chose to discretize space with four possible bin sizes: 2.0 m, 1.0 m, 0.5 m, and 0.2 m. These scales were chosen to represent the range, from large to small, that covered the limits of relevant accuracy. I chose 2.0 m because it is roughly equal to the achievable accuracy of many known building-sized BT localization systems [14, 17, 20, 26, 28]. I chose 0.2 m because I believe it is a reasonable lower limit on the desirable precision for the position of devices that are often on the order of 0.2 m in size. Any of these scales might be chosen as the scale for a real-world implementation of a system with discrete variables, and so presenting their results together still demonstrates a baseline of the capabilities of my model, rather than demonstrating the effects of varying a parameter.

In measuring the accuracy of the model at each of the four spatial scales, I chose five of the iMacs from the entire set of nine that will be used. The five iMacs chosen formed a diamond with one iMac in its centre, which I believe represents a variety of relative orientations. In the map in Figure 4.1, the five iMacs are numbered 7, 15, 18, 20, and 29. The generic procedure for evaluation described in §4.2 was therefore repeated five times: each time, one device was selected as the localizing device, and the remaining four were used as beacons, with

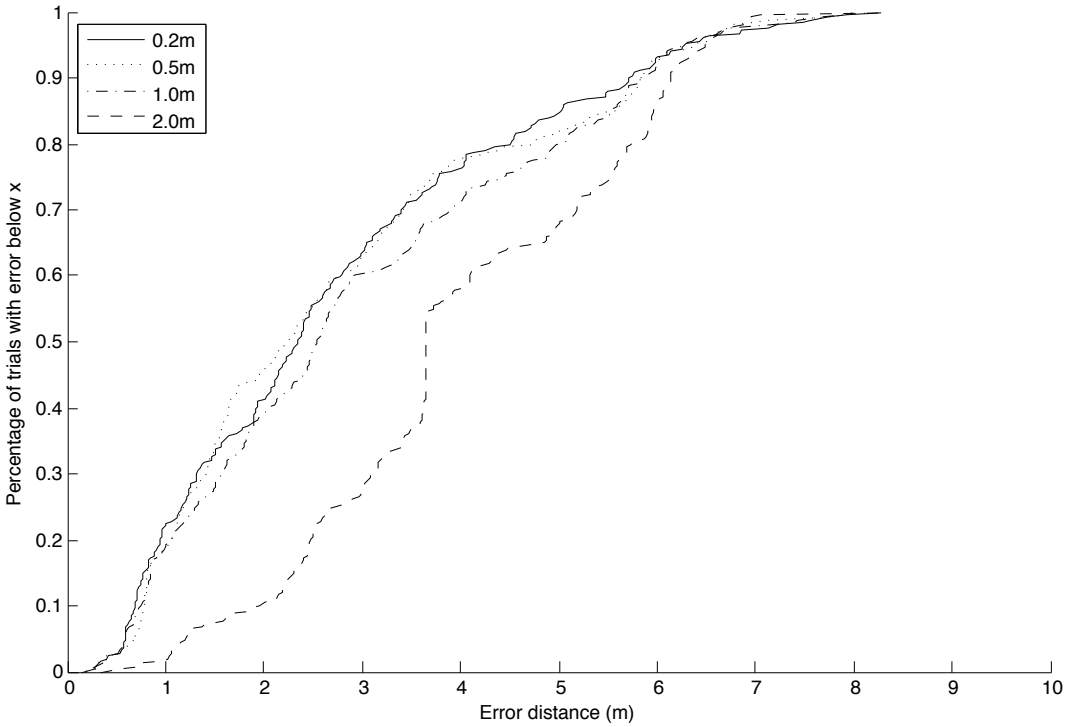

Figure 4.2: CDFs of distance error. Each curve represents a scale for discretizing space, and includes the results of localizing each of the five used iMacs. The Euclidean distance is evaluated from the mean of the position distribution. There are 250 trials per curve. The means and standard deviation of each curve are presented in Table 4.1a.

their known positions set as evidence in the network. As mentioned, the generic procedure also included another level of repetitions, drawing sample evidence from the gathered data 50 times to diminish any error due to the sampling procedure. Therefore, for each scale value, there are 250 instances of localization performed; for each localization device, there are 200 instances. Besides these two parameters, the default structure and parameters for the model were used, as described in Chapter 3. The only parameter choice was to use three signal strength readings per beaconing iMac.

In Figure 4.2, the 50% confidence level of the CDF of the error distance for all four scales is between 1 m and 2 m; the 80% confidence level for all four scales is between 2 m and 3 m. As the spatial scale decreases from 2.0 m to 0.2 m, the accuracy roughly increases. A subjective measure of this is how the area under the CDF rises by shifting the curve upwards and towards the left, such that more instances among the 250 trials in each curve have a smaller error. Subtable 4.1a also shows the means of each error CDF decreasing as scale decreases,

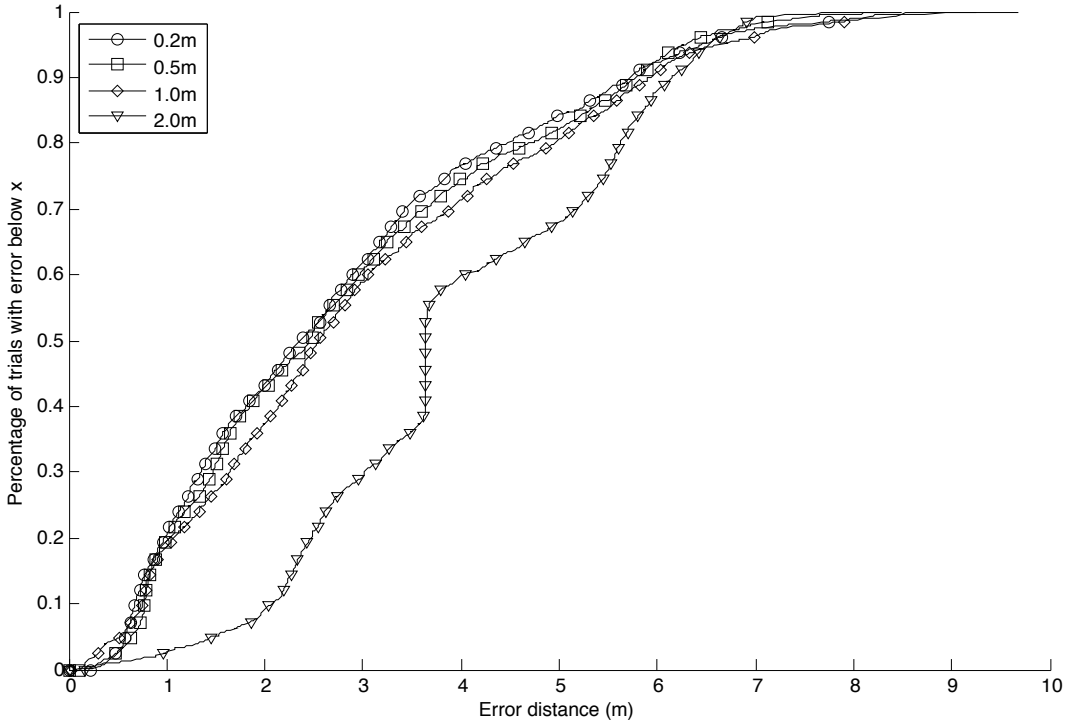

Figure 4.3: CDFs of distance error, using 250 trials per localizing device instead of 50 trials. Each curve therefore has 1250 trials. As in Figure 4.2, the Euclidean distance is evaluated from the distributions' means. The means and standard deviations of each CDF are presented in Table 4.1b.

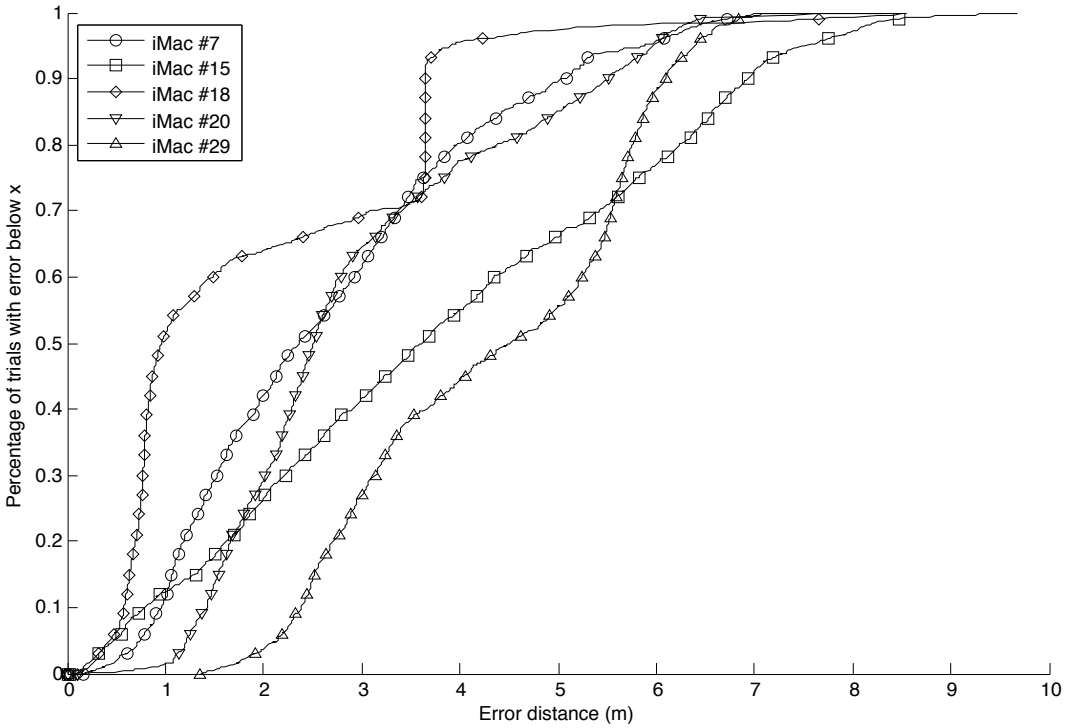

Figure 4.4: CDFs of distance error for 250 trials at each four scales, with each of five iMacs as the localizing device, grouped into CDFs by localizing device. The Euclidean distance is evaluated from the distributions' means. The legend is based on the iMac numbers as labelled in the lab. The CDF associated with iMac 18, the iMac at the centre of the five iMacs used here, demonstrates the highest degree of accuracy. The mean and standard deviations of each curve are presented in Table 4.1c.

from 2.7353 m with a 0.2 m scale to 3.98 m with a 2.0 m scale. As well, the amount that accuracy increases between scales roughly decreases as the scales decrease; that is, the rate of accuracy improvement decreases as spatial scale decreases. The difference in error between 0.2 m and 0.5 m spatial scales is less than that between 1.0 m and 2.0 m spatial scales. It is reasonable to conclude that at any of the chosen spatial scales, our model is capable of producing localization results with a level of accuracy that is comparable to the results published in the field. Gwon et al. [20], for example, report mean distance errors between ~ 5 m and ~ 2.5 m when comparing a variety of algorithms that used three BT beacons for trilateration. This leads us to the conclusions that trilateration with probabilistic calibration between distance and signal strength represents a valid technique; and that other conclusions drawn from my model, if they are independent of effects from using discrete variables instead of continuous ones, are broadly generalizable to other BT localization systems.

To explore the effects of the sampling method, Figure 4.3 contains the experimental results of a procedure with only one difference to that of Figure 4.2: the number of sampled signal strength trials is changed from 50 trials to 250 trials. It can be seen that the only change to the shape of the CDFs is to smooth them, but with no decrease in the error rate due to drawing more samples. This leads to the conclusion that the sampling technique for drawing signal strength readings is representative of the readings' original distribution, such that 50 trials present no significant sampling error. Unless otherwise mentioned, only 50 trials are used throughout the remainder of the experiments.

Figure 4.4 contains plots of the same data as in Figure 4.3, except reorganized such that each curve presents the results associated with choosing each of the iMacs as localizing device, at all of the four scales. It is presented here to demonstrate the effect of position among the beacons as a greater effect on localization accuracy than scale or other parameters that I later control for. This is important because, in a live situation, a device can be anywhere. For the purposes of designing a localization system, it could be useful to know optimal beacon organizations such that a device at every position in the environment can achieve minimal levels of error. However, when evaluating the ability of an arbitrary BT localization system to perform adequately under the influence of our chosen experimental parameters, one needs to isolate the effect of device location from the effects of the experimental parameters. To do

Scale (m)	μ (m)	σ (m)
0.2	2.7353	1.8873
0.5	2.7475	1.9105
1.0	2.9548	1.9341
2.0	3.98	1.6411

(a) Data for Figure 4.2

Scale (m)	μ (m)	σ (m)
0.2	2.7665	1.9149
0.5	2.8298	1.8803
1.0	2.9874	1.9895
2.0	3.9671	1.6035

(b) Data for Figure 4.3

iMac #	μ (m)	σ (m)
7	2.675	1.576
15	3.8396	2.2793
18	1.8788	1.563
20	2.9688	1.5072
29	4.3264	1.4891

(c) Data from Figure 4.4

		Localizing device				
		7	15	18	20	29
Scales	0.2 m	2.518625	3.784580	0.949556	2.765777	3.813971
	0.5 m	2.497070	3.693215	1.083463	2.817749	4.057525
	1.0 m	2.646204	3.250895	1.883058	3.327144	3.829757
	2.0 m	3.037969	4.629630	3.599282	2.964367	5.604183

(d) Mean error distances.

Table 4.1: Tables containing the means and standard deviations of each CDF in Figures 4.2–4.4. Specifically, subtables 4.1a–4.1c respectively contain the means and standard deviations of each CDF in order. Table 4.1d contains a two-dimensional table containing the means of the Euclidean error distances that make up the preceding CDFs, separated into separate entries for each localizing device and spatial scale combination.

this, all of the following experiments are repeated using each of the five iMacs as a localizing device. In this way, I incorporate the observed effects of device position that are present in Figure 4.4, but always with the combined accuracies of a variety of relative positions.

4.4 Limits to the Accuracy of a Model with Discrete Variables

4.4.1 Position within a Discrete Spatial Bin

There are a variety of ways that using a discrete model can impose artificial limits on the accuracy of the resulting query distribution. One example is that of rounding. As an example,

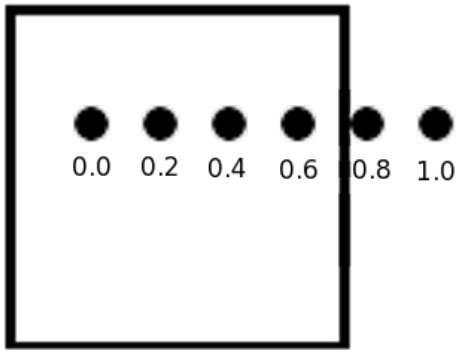

Figure 4.5: An example of how the devices were shifted for the experiment in §4.4.1. If a device started at the position labelled 0.0, it would have been shifted to each of the successive positions, where the labels represent the amount shifted in the X-dimension, in units of $1/5^{\text{th}}$ of the current spatial scale.

one can consider the case when the true position of a device is located on the divide between two spatial bins. A perfect localization system would place a peak of probability mass centred at the device. However, with discrete variables, the system must divide its mass into one of two nearby bins. Any evaluation method will attribute more error to the distribution than if the distribution had been continuous, because of the resulting dispersal of probability mass from the true position. As well, if a Euclidean distance is measured from the centre of one specific discrete spatial bin, the localizing device would have to be at precisely the centre of that bin for there to not be some error distance between the true position and the bin's centre.

To determine whether this had an effect on my analysis, I repeated localization having shifted the true locations of all devices by fractions of bin widths. In specific, I performed localization using the same five iMacs as in §4.3, repeating with each device as the localizing device and the other four as beacons, with three sampled readings per beacon, and repeated again with each of the four chosen spatial scales; this was repeated with 50 trials of sample readings. That process was then itself repeated six times: each time, the set positions of the four beacons and the known localization position used for evaluation were shifted in the X-dimension by 1/5 of the chosen spatial bin size. Thus, each iMac was present at some original place within a bin; was moved towards an edge of the bin it started in; crossed a bin division into another bin; and was moved further until it reached its original position, one bin over. By holding constant the distances between all five devices, I could continue to use

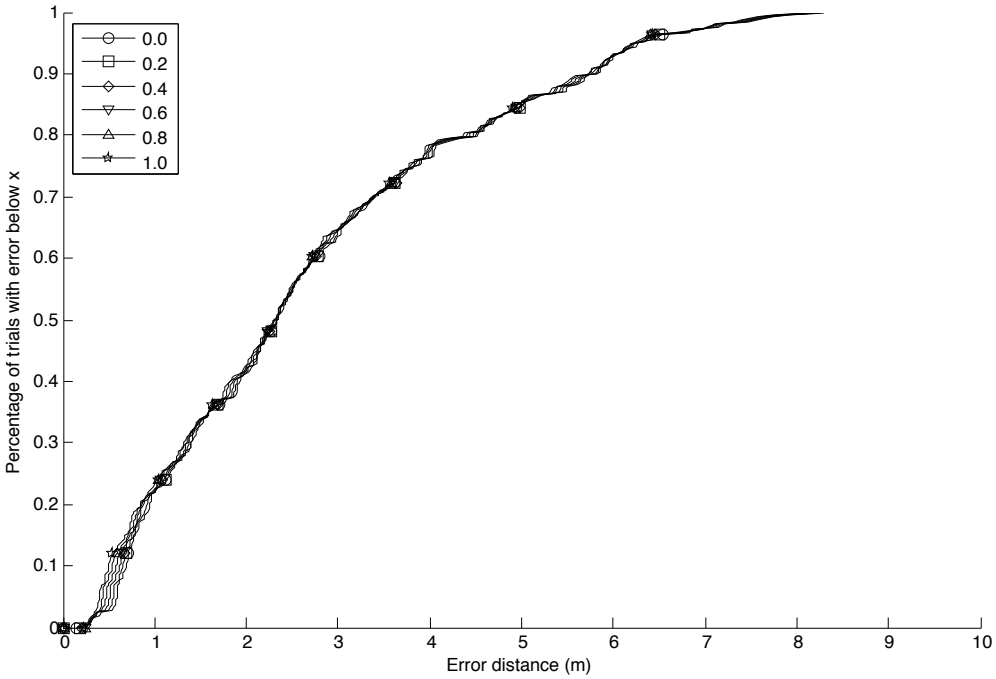

(a) Scale 0.2 m

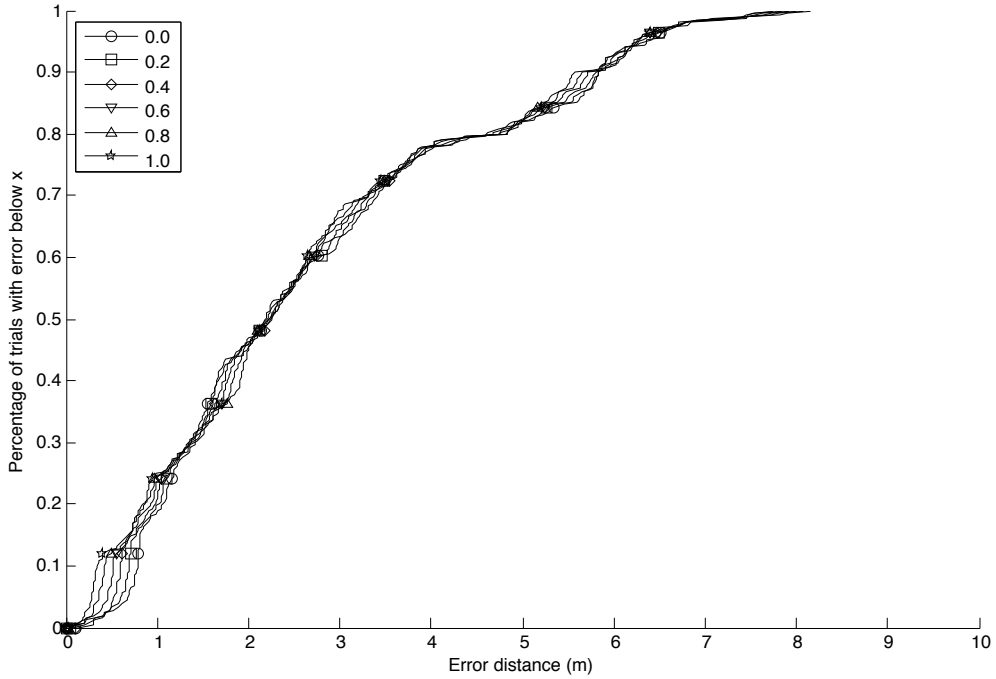

(b) Scale 0.5 m

Figure 4.6: CDFs of Euclidean distance errors from the mean of localization distributions for the experiments in §4.4.1. The results are divided into subfigures by spatial scale, beginning in Subfigures 4.6a–4.6b, and continued in Figure 4.7. The separate curves are each the result of shifting the positions of all five iMacs by equal amounts, as described in the text. The effects of rounding can be seen to increase from scales 0.2 m through 2.0 m, as the amount of rounding increases. Table 4.2 contains the means and standard deviations of each curve presented here and in Figure 4.7.

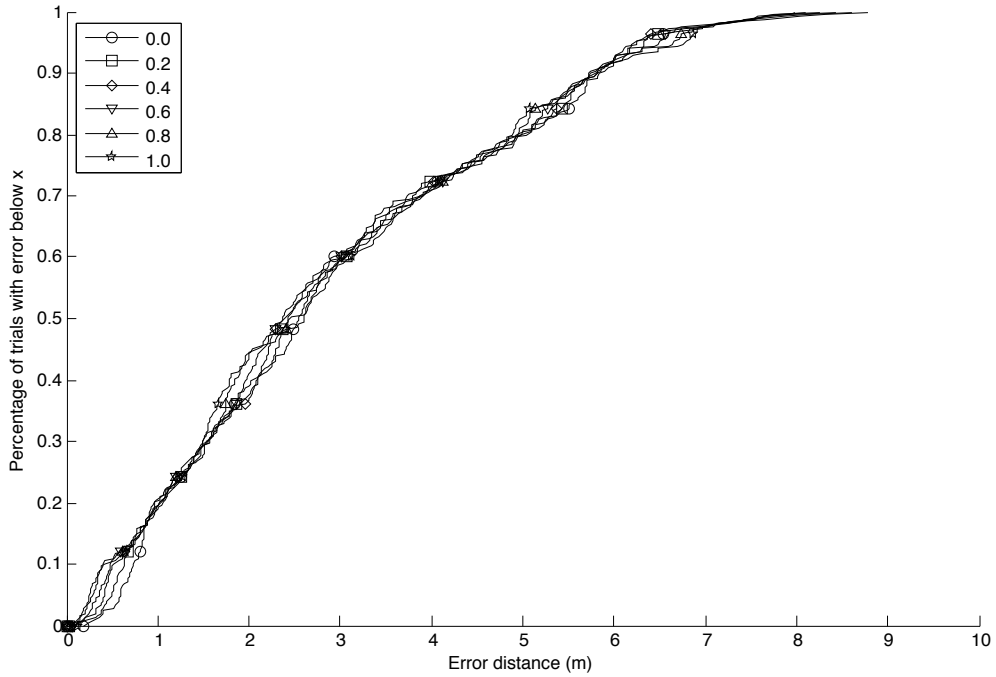

(a) Scale 1.0 m

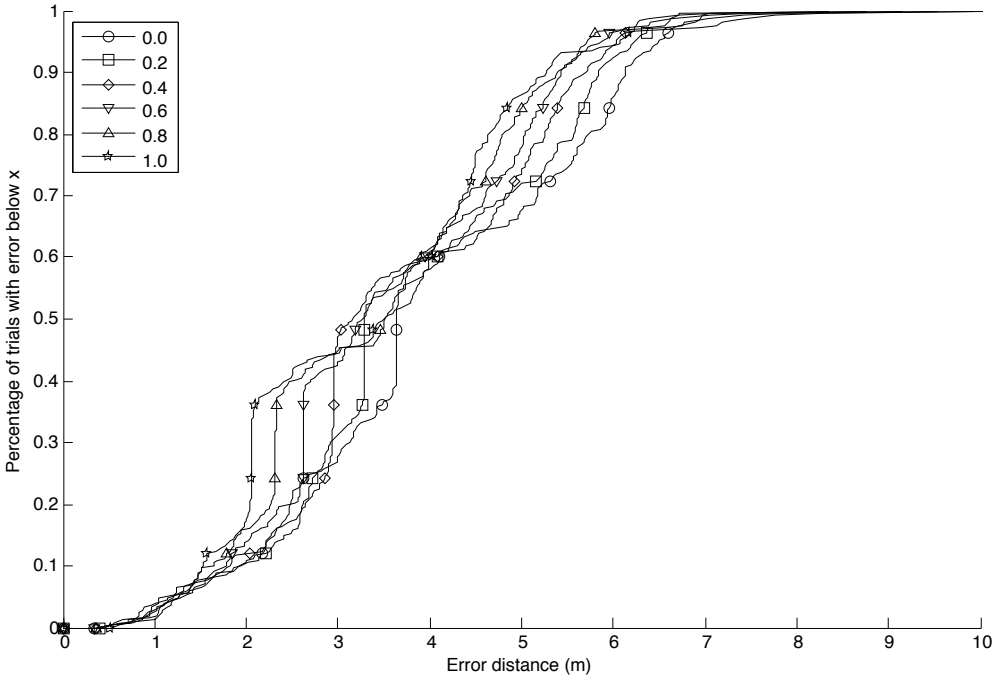

(b) Scale 2.0 m

Figure 4.7: Continuation of Figure 4.6. The data is presented in the same manner, for spatial scales 1.0 m and 2.0 m. The pattern of increasing effect continues as spatial scale size increases.

Shift	μ (m)	σ (m)
0.0	2.7353	1.8873
0.2	2.722	1.8887
0.4	2.7089	1.8904
0.6	2.6962	1.8923
0.8	2.6839	1.8946
1.0	2.6719	1.8971

(a) Scale 0.2

Shift	μ (m)	σ (m)
0.0	2.7475	1.9105
0.2	2.7206	1.9126
0.4	2.6963	1.9158
0.6	2.6745	1.9205
0.8	2.6557	1.9258
1.0	2.6405	1.9314

(b) Scale 0.5

Shift	μ (m)	σ (m)
0.0	2.9548	1.9341
0.2	2.9136	1.9511
0.4	2.8838	1.9708
0.6	2.868	1.9899
0.8	2.8712	2.0015
1.0	2.8934	2.0055

(c) Scale 1.0

Shift	μ (m)	σ (m)
0.0	3.98	1.6411
0.2	3.8204	1.5578
0.4	3.6804	1.5119
0.6	3.5624	1.5065
0.8	3.4688	1.5422
1.0	3.4012	1.6164

(d) Scale 2.0

Table 4.2: Tables containing the means and standard deviations for the CDFs in Figure 4.6. Each subtable is associated with one of the subfigures, based on spatial scale. The shift values are in units of fractions of the spatial scale.

the data recorded at their specific distances in the real world, without needing to construct signal strength readings to reflect the adjusted distances caused by shifting only a subset of the iMacs. Figure 4.5 presents an example of how a device would have been shifted relative to the bin it started in.

The results of this experiment are presented in Figure 4.6. The figure contains four subfigures, where each subfigure contains the data from each of the four chosen spatial scales. Each curve in the plots is the CDF of the Euclidean distance error from the mean of the resulting distribution, for one bin position. There are therefore six curves in each plot, with legend labels $\{0.0, 0.2, 0.4, 0.6, 0.8, 1.0\}$, in units of fractions of the current scale that the iMac positions were shifted.

At the scales of 0.2 m through 1.0 m, there is little to no variation between shift amounts.

It is therefore reasonable to conclude that at the discrete spatial scales of 0.2 m through 1.0 m, the position of a device within a bin has little effect on the accuracy of localization. At the scale of 2.0 m, however, there are areas of the curve where some differentiation occurs. This is likely due to the fact that more rounding happens with larger bins: when a device is on the boundary between two bins of the 2.0 m scale, the two closest bin centres are each approximately 1.0 m away instead of approximately 0.5 m away or less. At any of the chosen scales, however, the effect is small enough to not detract from the influence of other parameters in other experiments.

4.4.2 Proximity to the Edges of the Space

Another possible source of system-based error when using discrete, finite variables, is when the localizing device approached the boundaries of the environment. With edge-based error, probability mass can only occupy bin positions that exist. However, when a signal strength specifies a ring of probability at a distance value around a beacon, if that beacon is close to the edge of the environment then some of that ring does not exist. The probability mass that would be located outside of the boundaries of the system's represented space instead occupies bins that are proximal to the system boundaries, with a higher value after normalization than if the entire probability ring overlapped with the represented space. This has the potential to cause undue error when the distribution is evaluated: if two beacons produce signal strengths that would normally produce distance rings of approximately equal probability, but one beacon is close to the edges of the system, then that beacon is liable to skew the mean of the resulting probability distribution towards it, as more probability mass is centred around it.

To determine whether this was a system-wide contributing factor in my analysis of the error caused by varying other parameters, I performed an analysis similar to that in §4.4.1. In the case of system edge-based error, though, I translated the positions of the iMacs by the same value at all scales. This was because translating a device by a specific multiple of the scale 0.2 m did not make the devices approach the boundaries of the system. I therefore chose three increments of 2.0 m: 0.0m, 2.0 m, and 4.0m, to translate every device. As before, translating all five chosen devices by an equal amount allowed me to use the same

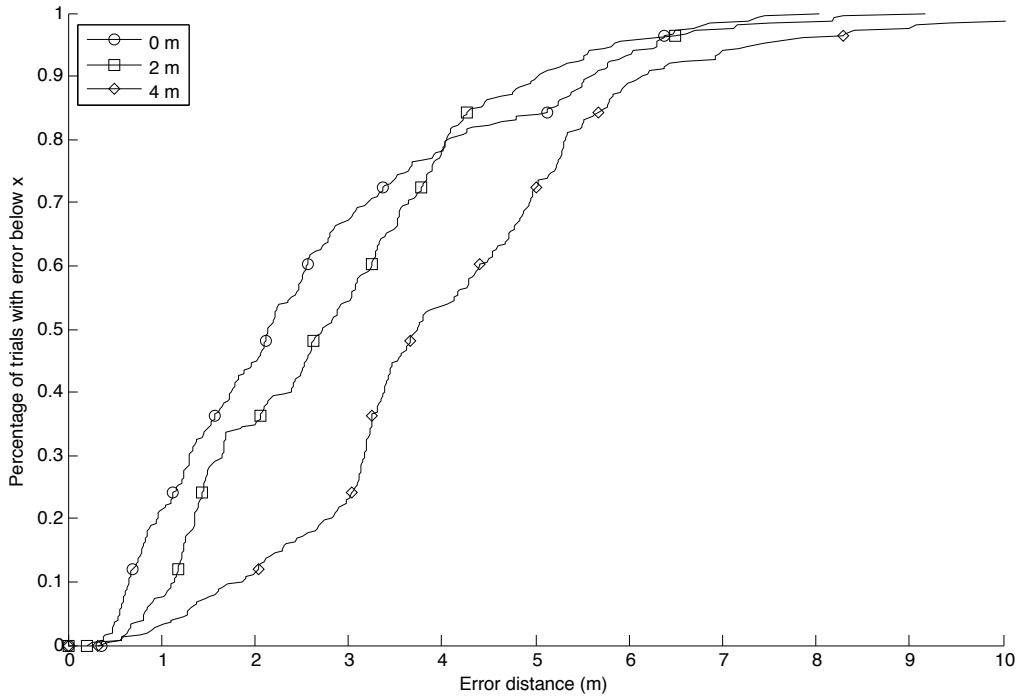

(a) Scale 0.2 m

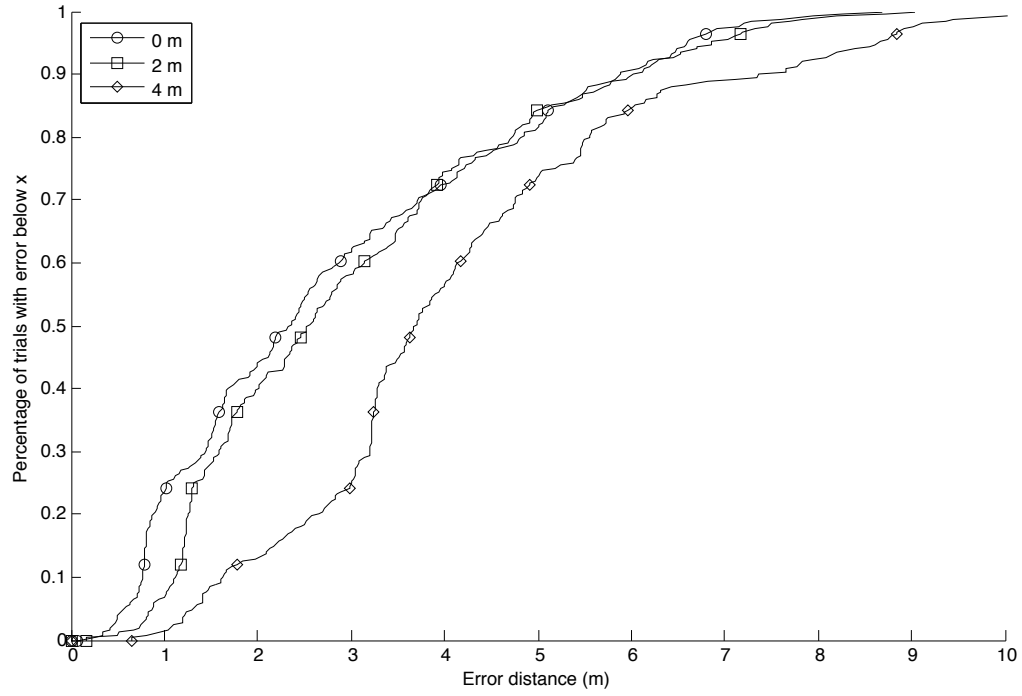

(b) Scale 0.5 m

Figure 4.8: CDFs of Euclidean distance errors from the mean of localization distributions for the experiments in §4.4.2. The results are divided into subfigures by spatial scale, beginning with Subfigures 4.8a–4.9b, and continuing in Figure 4.9. In each subfigure, the separate CDFs are each the result of shifting the positions of all five considered iMacs by equal amounts: 0.0m, 2.0 m, and 4.0m, labeled 0 through 2 respectively. Table 4.3 contains the means and standard deviations of each curve presented here and in Figure 4.9.

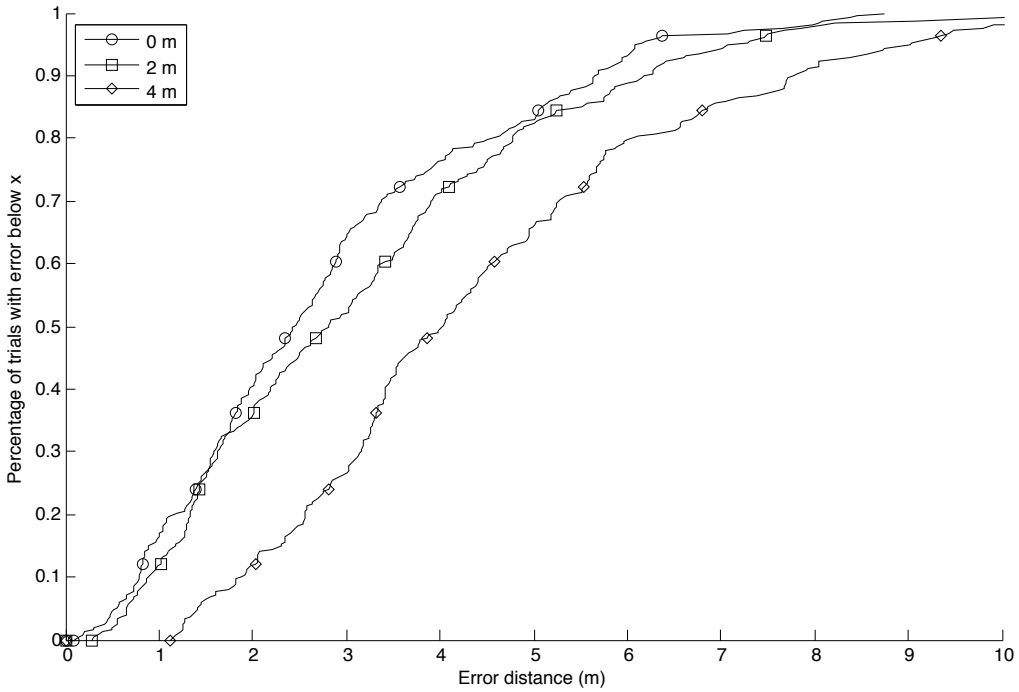

(a) Scale 1.0 m

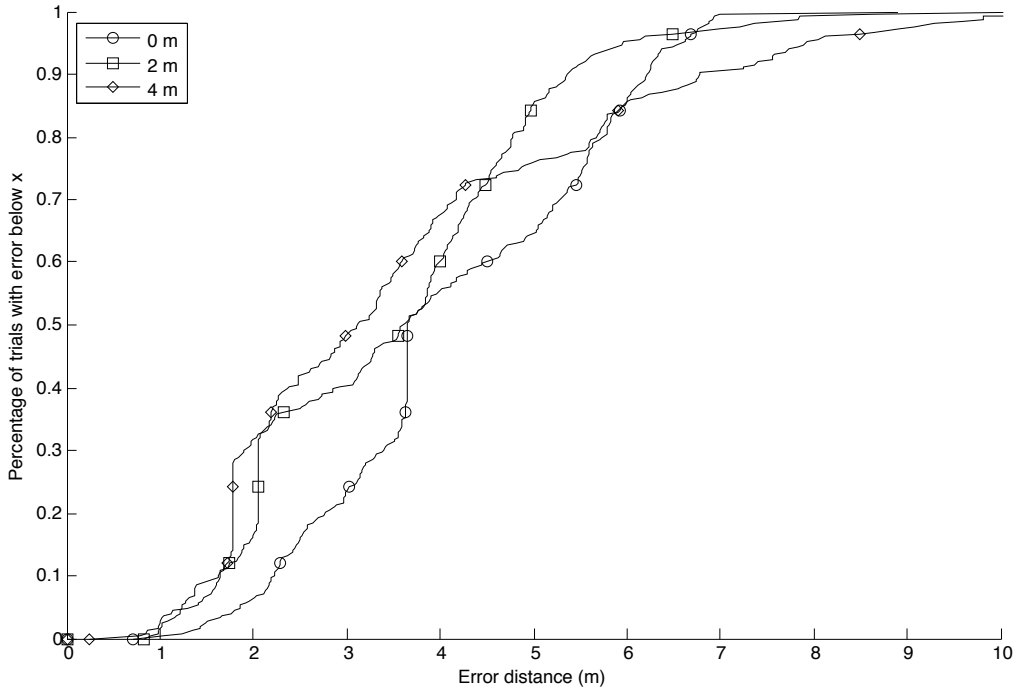

(b) Scale 2.0 m

Figure 4.9: Continuation of the results presented in Figure 4.9. The data is presented in the same manner, for spatial scales 1.0 m and 2.0 m.

Shift (m)	μ (m)	σ (m)
0	2.6209	1.8313
2	2.9054	1.6617
4	4.0836	1.8741

(a) Scale 0.2

Shift (m)	μ (m)	σ (m)
0	2.8342	2.0044
2	3.0169	1.9161
4	4.1474	2.0733

(b) Scale 0.5

Shift (m)	μ (m)	σ (m)
0	2.8349	1.8873
2	3.1743	2.0845
4	4.4692	2.2957

(c) Scale 1.0

Shift (m)	μ (m)	σ (m)
0	4.1603	1.5239
2	3.4965	1.6315
4	3.6384	2.2169

(d) Scale 2.0

Table 4.3: The means and standard deviations for each curve in Figure 4.8. The shifts are in units of meters.

gathered data, rather than fabricating new signal strengths for new distances between the devices. Another difference, however, is that in this case, not all of the devices occurred at all boundaries, in the way that every iMac approached and crossed a bin boundary as in the experiment with bin rounding error.

Figure 4.8 presents the results of these experiments. Each subfigure, 4.8a–4.9b, represents the results produced at each spatial scale, 0.2 m to 2.0 m respectively. Each curve is the CDF of the error results at each of the shifted positions.

The effect of moving the set of iMacs towards the edge of the system is more pronounced than the effects of moving a device within a bin. For example, at the 0.2 m spatial scale, the error measures varied by 0.06 m in the bin-shifting experiments, whereas at the same scale, the error measures varied by 1.4 m in these experiments. It is possible that the accuracy of a localization system could be negatively affected if it uses a finite and discrete representation of space, and if the devices in the system approach the edges of the localization space. [2] As

[2]The effect of moving devices within a finite space is still smaller than the iMac's position relative to the others, as presented in Figure 4.4. It is possible that some of the differentiation between the CDFs in Figure 4.4 is caused by a number of devices' proximity to the edge of the represented space. However, the general causes of differentiation in the results presented in Figure 4.4 are unknown, as the effects of the position of the localizing device relative to the beacons was unexplored.

well, at a spatial scale of 2.0 m, the effect of shifting the devices is inconsistent, suggesting that although there is some effect, it might not be entirely significant. For the purposes of the remainder of my experiments, however, the effects of being close to the edges of the space appears small enough that if I continue to repeat localization using each device as the localizing device and as a beacon for the others, the results of varying an experimental parameter will not be overly affected.

4.5 Limits to the Accuracy of BT Localization

4.5.1 Distance Calibration Levels

Another possible source of error is in the number of values chosen for our model of distance. The default model described in Chapter 3 used 2 m, 4 m, 8 m, and 12 m as values for the network nodes representing distance. These were initially chosen in designing the model because in our data gathering study, none of the devices were closer than 2 m, and the higher values represented a reasonable subset of the possible values in the range of useful RSSI readings. Because of BT's intended use as a short-range wireless communication, signal strength is unsuitably unstable as a measurement of distance beyond 10 m. Adding additional values for distance calibration has a cost in terms of computational time and space, as described in §3.1. These values were therefore considered reasonable as a default set of possibilities. However, my model's CPTs are encoded as a distribution over signal strength values for each possible value of the parent distance nodes. My signal strength calibration is therefore for these distance values only. Confining the set of distances that a measured signal strength could point to has the potential to limit localization accuracy.

This difficulty is not restricted to probabilistic models. Although the nature of a Bayesian network with discrete variables required me to choose calibration distances, non-probabilistic trilateration still requires gathering signal strength readings within the range of distances expected between devices. Blumrosen et al. [9] in particular had reasonable success at accurately determining the location of a BT device on a scale below a metre, by calibrating only at distances that small. On the other hand, most others [1, 2, 14, 17, 26] that include

calibration at distances lower than 2 m do not achieve error distances below 2 m more than 50% of the time. Because this increased error might be attributable to the fact that they do not calibrate extensively below 2 m, it is reasonable to conclude that, in some cases, calibrating more precisely than 2 m might allow a system to achieve more consistent levels of accuracy below this level.

To test whether the chosen number of values for the distance nodes were affecting the level of achievable accuracy in other experiments, I again repeated localization, but with a different number of possible distance values. In this experiment, I expanded the possible values from the default {2 m, 4 m, 8 m, 12 m}, to the more finely-spaced set {1 m, 2 m, 3 m, 4 m, 6 m, 8 m, 10 m, 12 m}. These new distance values were chosen to halve the original ranges of distance.

The calibration CPT values for the signal strength nodes given these distances, however, were not achieved by repeating the calibration data gathering procedure described in §3.5.1. Rather, recall that the calibration CPT distributions were formed by evaluating the equation for a log-normal distribution, using parameters of the mean and standard deviation of the gathered calibration data. For each new distance value from 3 m to 10 m, calibration data was constructed by shifting all gathered values for the following distance value by half of the difference between the means of the preceding and following values. (For example, for 3 m, the signal strength values gathered at 4 m were shifted upwards by half of the difference between the mean of the values gathered at 2 m and at 4 m.) For the new distance value 1m, calibration data was constructed by shifting the signal strength values gathered for 2 m calibration data, by 5 dBm. The value of 5 dBm was chosen because it was approximately equal to the shift value used for the 3m calibration data.[3] Given these new constructed sets of calibration data, the same process of calculating the mean and standard deviation and using them in a log-normal equation was performed in building the models used in the subsequent experiment.

[3]An extensive analysis of the validity of this constructed data was not performed. The method of choosing the midpoint between the means of two CPT distributions associated with two distance values is in fact inconsistent with the logarithmic relationship between distance and signal strength. The mean of a distribution for a distance midway between two existing distance values would in fact be slightly closer to the mean of the lower value than the midpoint between means. However, it is reasonable believe that another system might construct data in a similar fashion, and it is unlikely that choosing a more accurate set of calibration

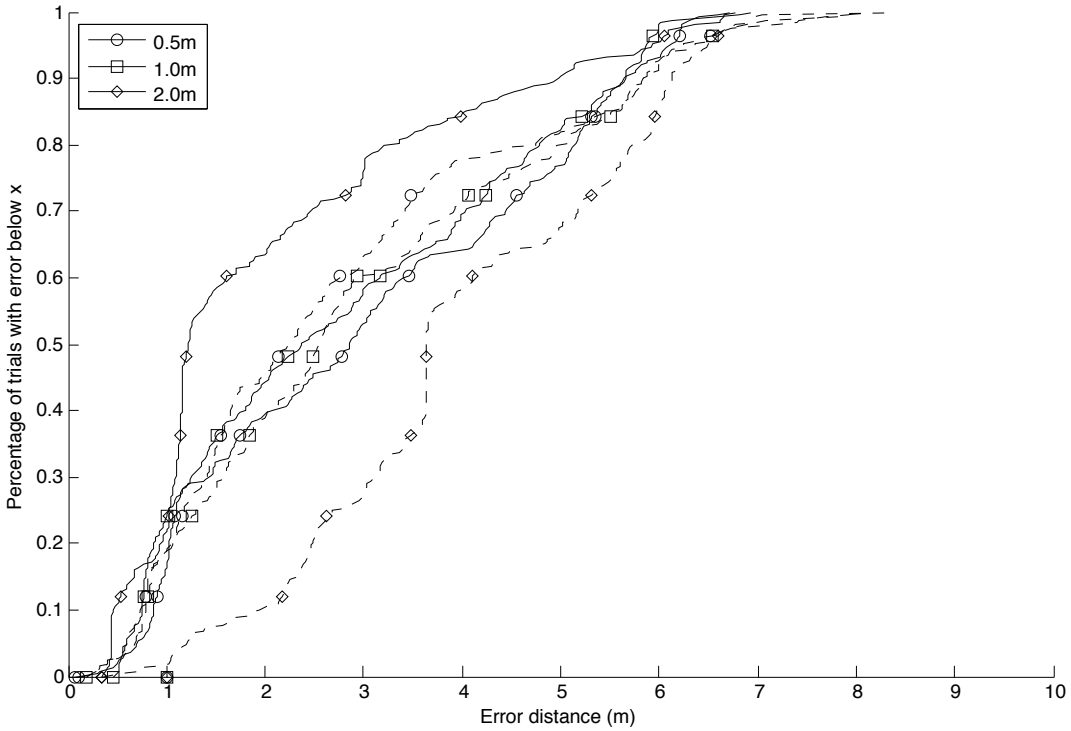

Figure 4.10: The CDF of distance errors from the mean of localizing distributions from networks using the expanded set of distance values. The expanded set of distance values includes 1 m, 3 m, 6 m, and 10 m distance values. Additional calibration was not performed: the CPTs of the signal strength nodes were generated based on adjustments to the calibration data for the default distance values. Table 4.4 presents the means and standard deviations of each curve.

As in previously mentioned experiments, all default model parameters were used, except for the number of distance values used, and the fact that spatial scale was varied. In this case, however, the 0.2 m spatial scale was excluded from results: the computer used for evaluation could not allocate sufficient memory, due to the combined effects of increasing the size of the spatial nodes and the distance nodes simultaneously. Localization was repeated five times using each of five iMacs as a localizing device and the remaining four as beacons. For each such model built with one set of parameters, signal strengths were sampled as evidence to the network, and the resulting distributions for the position of the localizing device were evaluated using the Euclidean distance from the mean of the distributions.

The results of this experiment are presented in Figure 4.10. As well, the results of the general accuracy experiments, presented in Figure 4.2, are repeated in the same plot, but with dashed lines instead of solid ones. (The 0.2 m scale of the general results are omitted because there are no results of this experiment at that scale.) Each curve represents the CDF of distance errors for a scale at which 50 trials and evaluations were performed. It can be seen that adding additional distance calibration levels has some effect on the accuracy of localization. There are three general trends.

- The maximum error decreased by adding distance calibration levels, as 100% of the trials occur at a lower level of error, below 7 m.
- At the 2.0 m spatial scale, the 50% error level is now below 2 m, and the curve for the 2.0 m scale in general has more instances with less error, as demonstrated by the curve moving to closer to the upper left corner of the figure.
- At the 0.5 m scale and 1.0 m scale, the effect to accuracy of adding distance calibration levels, other than lowering the maximum error, appears to be negligible.

The effects to localization accuracy are therefore not consistent at all scales. However, it is clear that additional distance calibration levels do influence localization accuracy, and in

data would result in less accuracy than observed. Therefore, the conclusions we reach from the associated experiments are not entirely unreasonable. To attempt to form some evaluation, however, we can compare the constructed data for the new 3 m distance value and one orientation, with data gathered between two iMacs that were 3 m apart and had that orientation. The distance between their means was less than the sum of their standard deviations.

Scale (m)	μ (m)	σ (m)
0.5	3.0301	1.8774
1.0	2.8056	1.8475
2.0	2.0732	1.6714

Table 4.4: The means and standard deviations of the CDFs presented in Figure 4.10.

some cases can drastically increase it.

4.5.2 Number of Beacons

Another source of error that a BT localization system faces is the number of beacons that the localizing device can detect. As discussed previously, traditional, non-probabilistic trilateration requires at least three BT devices as beacons to satisfy the associated system of equations in two dimensions. Among the research known to the author, only Fernandez et al. [15] studied the effects of using additional or fewer beacons. In their study, their BT localization system had four beacons, and they experimented with the accuracy of removing one of the four beacons from their localization and analysis. They reported that adding a fourth beacon increased the accuracy of their localization by 31% to 85%.

The flexibility of a Bayesian network to be expanded with additional nodes provides for two benefits over a hard-coded solution. The first benefit is that any number of beacons can theoretically be added to the system, barring implementation issues such as a lack of computer memory. A specific network can in fact be built on the fly during live localization with the appropriate number of beacons within range of the localizing device, an adaptability that would be difficult in a system that had to resolve the geometric issues of non-intersecting circles (see the work of Gwon et al. [20] described in §2.2). The second benefit is that, if a network is built in advance with more beacons that are not at runtime in range of the localizing device, the beacons can be ignored rather than removed by simply not entering evidence into their corresponding signal strength nodes. As described in §3.1, without the evidence of signal strengths to affect the distance between devices, the position nodes of the beacons are conditionally independent from the position nodes of the localizing device. With no signal strength values entered in evidence from a beacon, its influence is not transmitted

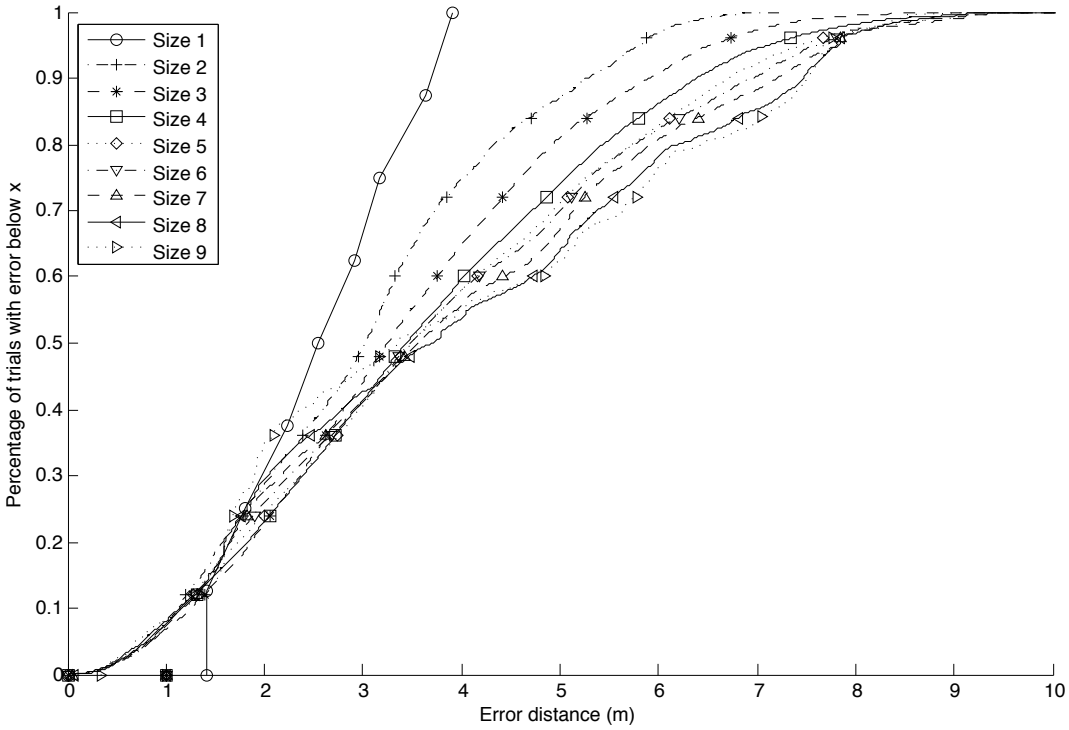

(a) Scale 0.5 m

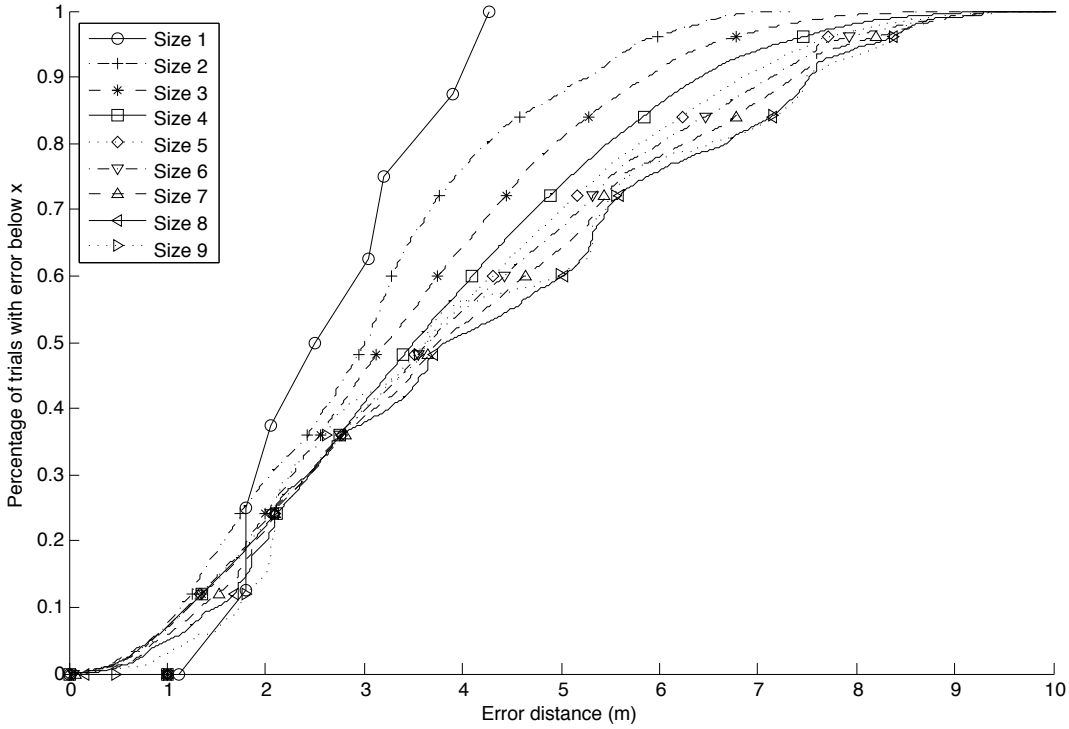

(b) Scale 1.0 m

Figure 4.11: 4.11a–4.11b

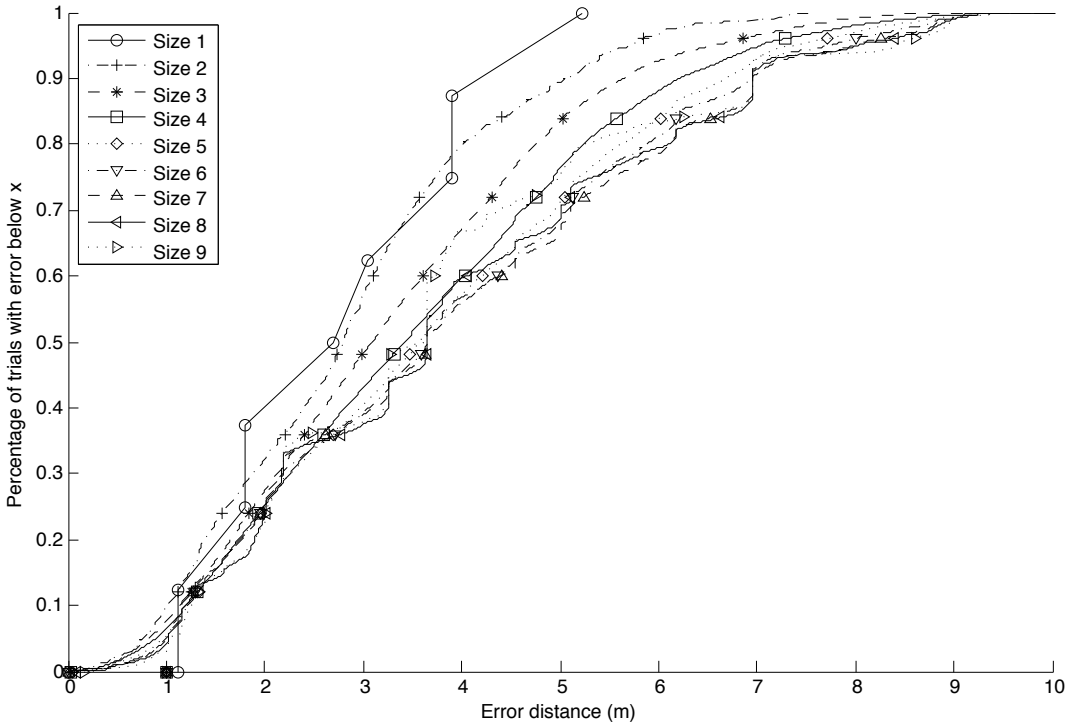

(c) Scale 2.0 m

Figure 4.11: The CDFs of the error distance from the mean of localization distributions using sets of devices of size 1 through size 9. Each CDF represents one of the three spatial scales, excluding the default spatial scale 0.2 m, which was not used because of memory requirements. The errors in the CDF for set size 1 are actually the evaluation metric applied to a uniform distribution, because localization with only one device provides no signal strength information. It is counter to results in the known literature that this produces more accurate results than the other set sizes. However, this is an artefact of the evaluation metric. The means and standard deviations of these curves are presented in Table 4.5.

by inference algorithms, and is effectively ignored.

To explore the effect on BT localization of both more and fewer beacons than in a typical trilateration system, I again performed a series of localizations, this time varying the number of devices used. Using all other default parameters, networks were built using sets of devices of size 1 through 9. For set size k, every possible combination of k of the nine possible devices was used. In the case of sets of sizes 2 through 9, as in the default procedure in §4.3, localization was repeated using each device as the localizing device and the other(s) as beacons. Localization was not actually performed for sets of devices of size 1: a set of devices of size one would have to include the localizing device, and therefore would include no beacons. With no beacons, there would be no influence on the prior distributions of the positional nodes of the localizing device. Therefore, the resulting distribution would always be uniform, as I have designed my model with no prior information as to the positions of devices. The mean of the distribution for set size 1 was therefore assumed to always be the centre of the room; the error distance is the Euclidean distance between the localizing device's true position and the centre of the room.

The results of evaluating these uniform distributions is included in the CDFs presented in Figure 4.11. As before, for a network with a fixed set of parameters and beacon positions, localization was repeated with 50 different combinations of sampled signal strengths. However, in the case of Figure 4.11, because the error results are grouped by the number of devices that the network represents, the number of cases represented by each CDF varies. The number of localization trials performed in each CDF curve is given by the function:

$$\text{Trials}(k) = 50k\binom{9}{k} \tag{4.5}$$

where k is the chosen set size. This is why the smoothness of the curves varies among set sizes: because the smaller and larger set sizes have fewer trial results included in their curves, following the shape of a binomial distribution.

An important result in Figure 4.11 is that the results of localization with one device are apparently more accurate than any other amount of devices; that, counter to the results presented by Fernandez et al. [15], accuracy *increases* as set size *decreases*. For example, at the 1.0 m spatial scale, localization error increases from 2.6 m with set size 1 to 4.16 m

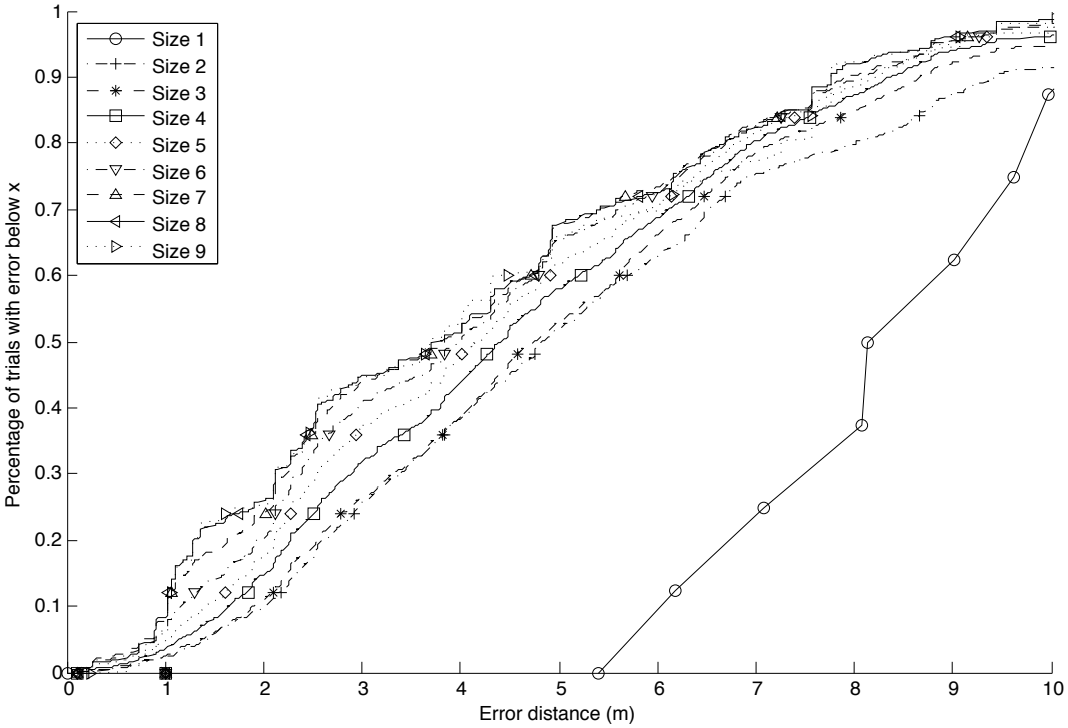

(a) Scale 0.5 m

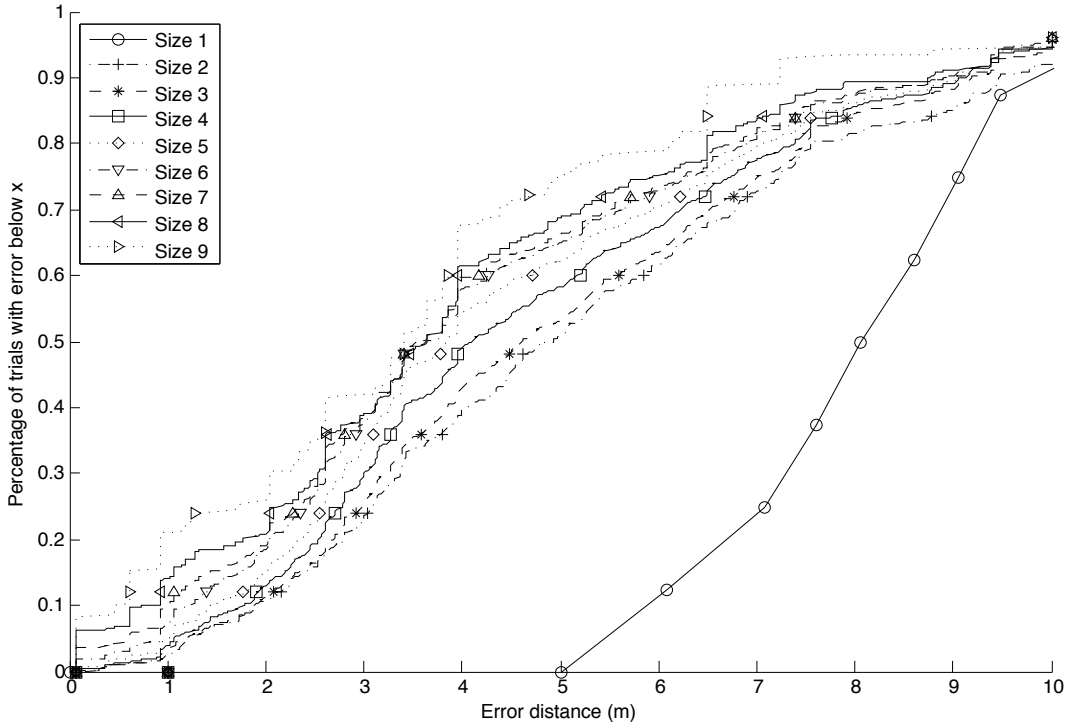

(b) Scale 1.0 m

Figure 4.12: 4.12a–4.12b

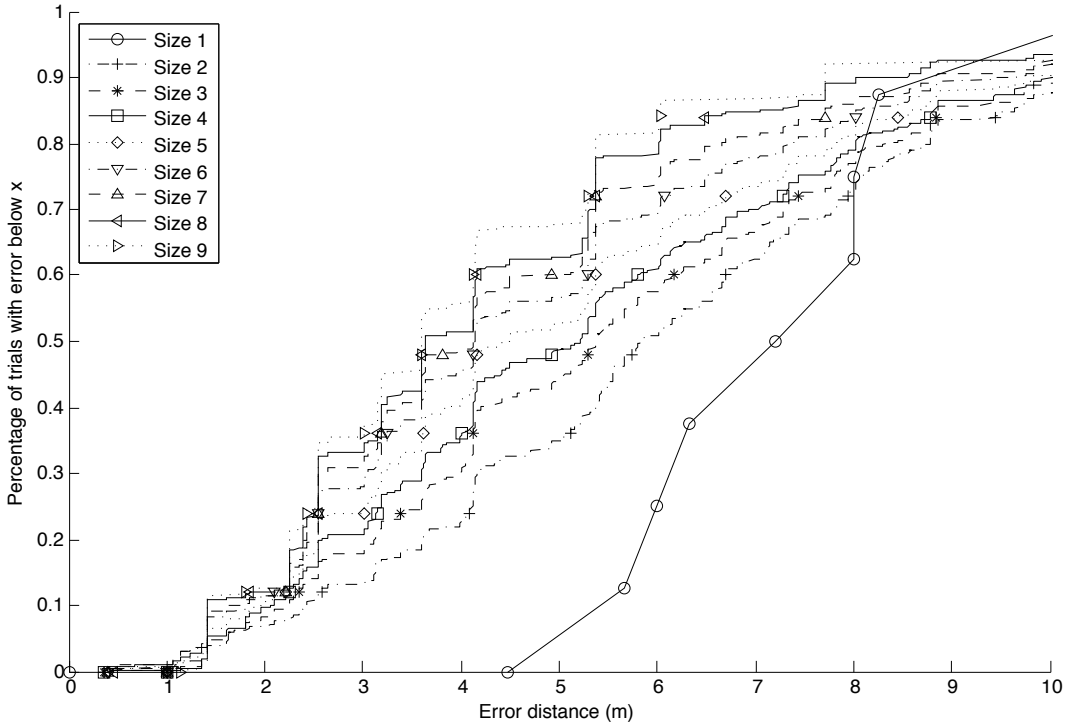

(c) Scale 2.0 m

Figure 4.12: The CDFs of the Euclidean distance error taken from the maximum of the same localization distributions as were evaluated in Figure 4.11. Evaluating from the distribution maximums in this case demonstrates a proportional relationship between the number of devices used and the accuracy of localization, that was not apparent when the distributions were evaluated from their means.

Set size	μ (m)	σ (m)
1	2.56	0.91985
2	3.0509	1.5119
3	3.4337	1.7341
4	3.6651	1.9643
5	3.773	2.0933
6	3.7901	2.1474
7	3.8685	2.2356
8	3.9494	2.3339
9	3.8988	2.4132

(a) Scale 0.5

Set size	μ (m)	σ (m)
1	2.6339	1.0496
2	3.0315	1.5047
3	3.4137	1.7597
4	3.7112	1.961
5	3.8671	2.1026
6	3.9502	2.185
7	4.0942	2.2395
8	4.2366	2.2997
9	4.1581	2.2676

(b) Scale 1.0

Set size	μ (m)	σ (m)
1	2.734	1.4132
2	2.8671	1.5131
3	3.2845	1.7542
4	3.5952	1.9322
5	3.7698	2.0541
6	3.8699	2.1436
7	3.9241	2.2308
8	3.9066	2.1909
9	3.7414	2.1403

(c) Scale 2.0

Table 4.5: Tables containing the means and stand deviations of the CDFs in Figure 4.11.

with set size 9. This can be attributed to a combination of the evaluation method used and the structure of the space used for data gathering, rather than to an effect of the number of beacons used. As described, querying a model built to represent only one device will always return a uniform distribution. The mean of this distribution will then always be at the very centre of the represented space. Because this is where the iMacs used for data gathering were actually located, the centre of the room is a fairly accurate guess given no other information. In effect, any attempt at localization, when evaluated using the mean of the resulting distribution, is liable to be more accurate simply because the original position of the iMacs was close to the centre of the room.

To demonstrate that the problem is the evaluation method and not that localization is less accurate than a uniform distribution, I can instead evaluate the results of localization with every possible set size, using the Euclidean distance between the maximum of the distribution and the true iMac location. As discussed in §4.2.1, this method of evaluation will include less information about the overall shape of the distribution, and will focus directly on only the single spatial bin believed to be most likely. Localization was repeated using the exact same signal strengths that were randomly sampled and used for localization to create

Set size	μ (m)	σ (m)
1	8.2951	1.8617
2	5.2999	2.8326
3	5.0532	2.6163
4	4.7403	2.5905
5	4.4955	2.5854
6	4.2959	2.5963
7	4.1388	2.631
8	4.0711	2.615
9	4.1654	2.694

(a) Scale 0.5

Set size	μ (m)	σ (m)
1	8.0174	1.8537
2	5.3511	2.9163
3	5.128	2.774
4	4.8494	2.7475
5	4.6055	2.7545
6	4.3828	2.7608
7	4.2884	2.8018
8	4.1181	2.8012
9	3.6538	2.6399

(b) Scale 1.0

Set size	μ (m)	σ (m)
1	7.1868	1.8422
2	6.2275	2.9725
3	5.7902	3.0353
4	5.5259	3.0126
5	5.2715	3.0151
6	4.9921	2.9884
7	4.7759	2.9446
8	4.5167	2.7962
9	4.3441	2.8374

(c) Scale 2.0

Table 4.6: Tables containing the means and stand deviations of the CDFs in Figure 4.12.

Scale (m)	μ (m)	σ (m)
0.2	3.533	2.5749
0.5	3.675	2.3782
1.0	3.88	2.4297
2.0	3.6258	2.3721

Table 4.7: The means and standard deviations of each curve in Figure 4.13.

the CDFs of Figure 4.11. Localization would therefore produce the same distributions; the results of evaluating from the maxes of these are presented in Figure 4.12. For comparison, I present in Figure 4.13 the same results of localizing with the model's default parameters, as was presented in Figure 4.3, but also evaluated from the maximums of those distributions. Figure 4.13 also contains the results of Figure 4.3, drawn with dashed lines instead of solid lines. The same scales in both cases have the same colours.

At all scales, a set of devices of size one now underperforms relative to the other set sizes. For example, at spatial scale 1.0 m, accuracy decreases from 8.02 m with set size 1, to 3.65 m with set size 9. This is because in the case of multiple bins in the localization distribution having identical values, the bin closest to $\langle 0, 0 \rangle$ in X and Y is chosen as the maximum: that

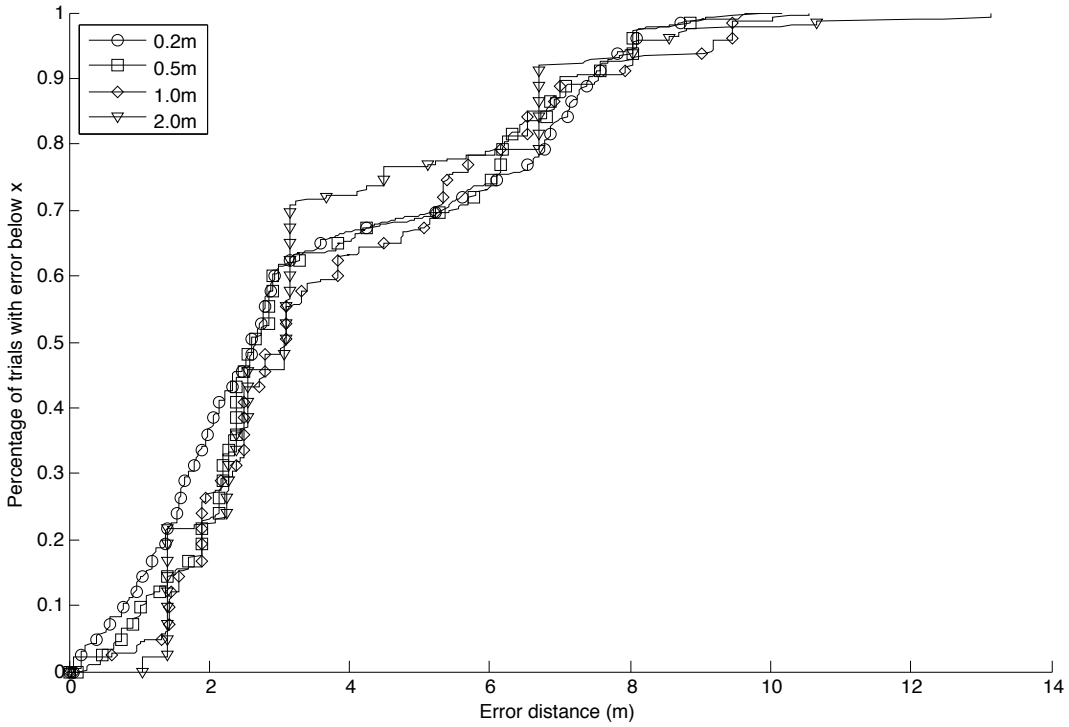

Figure 4.13: CDFs of distance error for the same distributions as were evaluated and presented in Figure 4.3. The Euclidean distance reported in the solid curves is evaluated from the maximum of the position distribution; in the dashed curves, it is evaluated from the mean of the position distribution. The means and standard deviations of the solid curves are presented in Table 4.7.

is, rather than calculating the Euclidean distance between the true iMac location and a point at the centre of the space, distance is calculated between the true position and the corner of the room. The results for a set size of one are still biased by the evaluation, though, as the corner of the room is no more representative of the entire uniform distribution than the centre of the room.

The other effect of evaluating localization based on the maximum of the resulting distribution is that accuracy increases with set size, rather than being inversely proportional. This is as expected from the report of Fernandez et al. [15]. However, it is important to note that there are diminishing returns with increasing set size. The decrease in error between set sizes of 3 and 4 are somewhat distinguishable in Figure 4.12, but it becomes much less so beyond a set size of 5 or 6. As well, the difference between set sizes of 2 and 3 are smaller than one might expect, given that a non-probabilistic trilateration system requires three beacons. Other BT localization systems might benefit from taking an opportunistic stance: if an environment has an inconsistent beacon density, being able to include signal strength readings from more beacons if they are available could increase accuracy; as well, localization with fewer beacons than three still has the potential to be satisfactorily accurate for some applications.

Chapter 5

Conclusion

5.1 Discussion

In Chapter 4, I described the experiments I performed to explore how position within a bin, proximity to the edges of the localization space, the number of beacons used, and the distance calibration levels could potentially influence the accuracy of a BT localization system. It is worth emphasizing, however, that the BT localization system used for this analysis was unique among the known literature for the following reasons: for using discrete variables in its model of localization; for using iMacs as the beacons and localizing devices; for representing trilateration calibration probabilistically; and for using Bayesian inference algorithms to combine multiple signal strength readings from the same beacon into a single distance estimation between the beacon and the localizing device.

Using discrete variables in my model was in large part what allowed me to experiment with the parameters. However, the differences between continuous and discrete variables could have affected our results. This is why I undertook the experiments to determine if bin position and edge proximity were factors in localization accuracy. The results of the bin position experiment indicated that if discrete variables are used to partition space into bins of sizes between 0.2 m and 2.0 m, there is little to no effect from a device's position within a bin.

The edge proximity experiment, on the other hand, indicated that there was some effect to localization accuracy when a localizing device was closer to the edge of the represented space. However, this effect was inconsistently observed, and was demonstrated to be a smaller effect than that of the position of a localizing device relative to the beacons. In general, for a BT localization system with discrete variables, it would be beneficial to place beacons

such that the ring of probability mass that forms around them (see Figure 3.3) is contained within the represented space rather than outside of its boundaries; and also, to choose a represented space such that the localizing device would be most likely positioned away from the boundaries of the space. To achieve this artificially, those that are implementing such a system could choose to add a buffer of X and Y values outside of the range that actually exists in the intended localization environment. As discussed, though, increasing the size of the represented space has drastic effects on the memory and computational requirements of a discrete valued Bayesian network and inference algorithm.

In general, because a localization system cannot enforce that the localizing device remain at the centre of the localization environment, the effects of a device's proximity to the edges of the represented space cannot be controlled for in a practical system, and can only be reduced in offline experimentation by including devices at a variety of positions. Because of my results in Figures 4.2–4.4, it is reasonable to conclude that although edge proximity can affect localization, it does not significantly diminish the accuracy of my results compared with previous results. Further, because of the limited effect observed due to the position of devices within a bin, it is reasonable to conclude that my choice to model BT localization with discrete variables does not preclude my results from being generalizable.

As discussed in §2.2, Blumrosen et al. [9] demonstrated that localization with accuracies below 1m was achievable after calibration at the same scale. I also showed in §4.5.1 that calibration using additional distance values could affect the accuracy of localization. It is important to note, that the calibration I used in my model for this experiment was constructed by modifying the calibration at other distances. It would be beneficial to have confirmation of my results, that empirically repeats the calibration process at all used distance values.

However, an issue with calibrating at distances below 1m is that the iMacs are approximately 50cm wide. If the calibration is to still include orientation, signal strengths would have to be gathered with the iMacs facing in all combinations of orientations at distances below 1m. This includes the combination of orientations where the iMacs are in-line with each other (as in Figure 3.5), and so the minimum possible distance value becomes double the largest radius from the iMacs' centres, because the iMacs could not physically move closer to each other. If the best consistent accuracy is limited to the smallest calibration dis-

tance used, then it is possible that the physical size of the beacons used could be the lowest possible resolution of a BT localization system. Although iMacs were chosen as a typical BT-equipped device that might be encountered in a localization environment and could thus be used for localization without requiring additional infrastructure to be deployed, many other common devices are now equipped with BT, such as laptops, printers, and the vast majority of smartphones. Every device will have its own pattern of attenuation and resulting signal propagation around it. Large devices used for beacons have a greater potential to require angle-based calibration, and therefore also a greater potential to restrict the smallest level of distance value used for calibration; smaller devices used as beacons, on the other hand, have a greater potential to be mobile themselves. For example, Symington and Trigoni [47] describe a method for using distance estimates measured between multiple localizing devices during encounter events to improve on their individual tracking estimates.

The other experiment I undertook that could be generalized to BT systems that don't use models with discrete values, was to study the effect of the number of beacons used in localization. I found that localization accuracy did increase as the number of beacons was increased. I also found that using only two beacons or only one beacon reduced the accuracy of localization, but not as drastically as prior research would lead one to believe. The majority of trilateration systems limit themselves to exactly the number of beacons required for the standard formulations of the problem. The benefits of either using fewer beacons in the face of a system with sparsely deployed devices with the cost of only a slightly reduced accuracy, or opportunistically using more beacons if the situation presents itself, are therefore a direct side effect of my use of a probabilistic calibration and Bayesian inference to reason from signal strengths to a probability distribution of locations. Although I did not here demonstrate that localization accuracy increased from a probabilistic calibration alone, it would likely be worthwhile for the field to further explore the potential benefits of probabilistic trilateration modelled by Bayesian networks.

5.2 Recommendations

To future implementations of indoor localization systems that use BT RSSI to estimate distances for trilateration, my most emphatic recommendation is to use a probabilistic calibration of signal strength to distance. When two BT devices are placed at a fixed distance apart, the signal strength reading between them is never a single fixed value, but rather a distribution of possible signal strengths from which instantaneous readings are drawn. A probabilistic model of signal strength versus distance is simply closer to the truth of the relationship between the devices' transceivers, the distance between them, and the signal strength they observe; and any other model, when correct, is merely lucky.

Given a probabilistic calibration of signal strength versus distance, however, there are two readily conceivable options for implementing an indoor localization system. The two options are either to replace the calibration equation

$$s_i = a - b \log r_i \tag{5.1}$$

originally presented as equation 2.2, with the equation

$$r_i = \arg\max_d \mathrm{P}(D = d \mid S = s_i), \tag{5.2}$$

using the probabilistic model to determine a distance estimate for a non-probabilistic version of trilateration; or to incorporate $\mathrm{P}(S \mid D)$ into a larger probabilistic model such as a Bayesian network, as was done in the work described in this thesis document. I recommend the latter, because of the benefits to incorporating the information from beacons that this method provides. In specific, a Bayesian network avoids issues of resolving intersection points in the complex plane, as described in Gwon et al. [20]. As previously mentioned, an inference algorithm will combine the information of signal strength readings and beacon positions to influence the posterior position distribution, obviating the task of solving a closed-form system of equations. The other important benefit of using a Bayesian network to model the distance combining aspects of trilateration is that any number of beacons can be used. As demonstrated in §4.5.2, the number of beacons used can have an effect on localization accuracy. By allowing a BT localization system to incorporate a variable number of beacons, the system can respond to an abundance or dearth of in-range beacons appropriately.

Another recommendation would be that if a probabilistic model of BT localization is to use discrete spatial variables, then it should provide a means of reducing the effects of proximity to the edges of the space, as demonstrated in §4.4.2. This should be given some consideration, as merely adding a buffer of spatial values outside of the original scope can drastically increase the memory and computational requirements of the model. Alternatively, care should be taken in the deployment of beacons such that they are central to the represented environment, if this is feasible given the usage of the space.

Also, I would recommend gathering calibration data at as many distances as possible when implementing a BT-based trilateration system, including at the intended lower limit to resolution. Blumrosen et al. [9] demonstrated a BT trilateration system with a resolution on the order of a few centimetres, but it is not clear if the increase in resolution was due to the increased proximity of their localizing device to their beacons (42.42 cm apart). In this thesis document, I also demonstrate that a combination of the lowest calibration value and more distance calibration levels can affect the accuracy of localization. Although it is not clear in either case that other factors were not conflated with the effects of the lowest calibration value, lowering the smallest distance value is the consistent element in both cases.

5.3 Summary of Conclusions

The following are the conclusions reached through the research done for this thesis document.

- When performing indoor trilateration with BT beacons, a probabilistic calibration between BT signal strength and the distance between localizing device and beacons can result in location estimates that are accurate enough for a number of the indoor localization applications cited in the literature. The accuracy of my model when built with generic parameter values is roughly the same as the accuracy of other known systems.

- When performing indoor trilateration with more than four BT beacons, the accuracy of localization increases as more beacons are added.

- When performing indoor trilateration with two BT beacons, localization with two BT beacons is not significantly less accurate than localizing with three BT beacons.

- When performing indoor trilateration with BT beacons, using additional discrete distance values and a smaller lowest distance value can increase the accuracy of localization at some sizes of discrete spatial bins. This effect was most prevalent at the largest used discrete spatial bin size of 2.0 m. At the other sizes of discrete spatial bins used in my experiments, more and smaller distance values can lower the maximum localization error, and have the potential to also increase accuracy under other circumstances.

- When modelling indoor BT trilateration using discrete variables, the position of the devices within the spatial bins does not significantly affect the accuracy of localization.

- When modelling indoor BT trilateration using discrete variables, the proximity of the devices to the edges of the localization environment can decrease the accuracy of localization.

5.4 Future Work

5.4.1 Rigorous Cost-Benefit Analysis

In §3.1, I explained how the growth rate of the time and space requirements of a Bayesian network with discrete variables grows exponentially with the number of values of some of the variables in the network. Although there are optimizations available to mitigate this expense for implementations in the field, they were not applied in the experiments described in Chapter 4. For example, nodes in the network that are neither query nodes nor in evidence can be compiled into the run-time model using a process called "absorption" [45]. Absorption is essentially a way to marginalize out so-called nuisance parameters: when a node is absorbed, it is no longer present in the network, and therefore its CPT is not a part of the factorization of the joint probability distribution; however, the process maintains the information contained in its CPT in other CPTs of the resulting network. Maintaining the original structure of a network without any modifications allowed me to have full control over the structure of any network built in my experiments, and thus to explore the benefits of a variety of possible parameterizations.

However, the costs associated with those benefits were never adequately measured. For example, the space requirements for performing localization with all possible combinations of nine devices were extreme enough that memory swapping to disk occurred when computations were run on a computer with 8GB of RAM, and a machine equipped with 256GB of RAM was instead used to perform the evaluation in a more timely fashion. The purpose of these experiments was to determine how known variables affected localization accuracy, free of constraints such as limited memory, and so neither the total memory usage nor the computation time were ever measured precisely. The same experiments as described in Chapter 4 could be performed again, but instead with appropriate profiling tools so as to measure the memory and computation costs associated with each parameter variation. These experiments could be performed without optimizations, and also with sufficient modification as to allow the network to be constructed within the memory requirements of a mobile phone, if possible.

5.4.2 Modelling Impedance through Obstacles

The networks I built modelled the effect of device orientation to signal propagation, which is not done in the prior literature. The strategy of leveraging Bayesian networks' conditional probabilities to desribe distributions of one variable given those that influence it, could be extended to describe other features of BT localization. For example, one of the most cited sources of error in BT localization systems is the effect of obstacles on signal propagation. Any walls within the environment have the capability to transmit the RFEM waves used by BT, but a small amount of signal strength loss is incurred as the RFEM wave travels through the object. This affects the associated estimate of distance.

It is feasible that this behaviour could be modelled explicitly. If calibration was performed with data that was taken in the localizing environment, the collected readings would include some that were affected by the obstacles in the area. In this way, any calibration would implicitly combine the conditions of line of sight transmission and transmission through an obstacle, into one probability distribution or set of fixed calibration parameters. To extend calibration to explicitly include transmission through an obstacle would involve gathering signal strenghts, instead of at every combination of distance and orientation, at every combination of distance, orientation, and transmission medium (that is, a binary variable of

whether the signal passed through an obstacle or not). When a low RSSI is received from a beacon, the network's automated reasoning algorithm would then have three possible explanations for the low reading: an increased Euclidean distance between the devices, a relative orientation with high impedance, or a decrease in signal strength due to the impedance of an obstacle. The network could then be better equipped to localize accurately when presented with a signal strength that would otherwise disagree with the position implied by non-impeded signals from other beacons.

5.4.3 Temporal Tracking with a Map-based Transition Model

In §2.3, I discussed the methods for performing temporal tracking using Markov chains, a subclass of Bayesian network. When localizing using trilateration, these systems apply these Bayesian techniques to the results of non-probabilistic trilateration. Rather than modelling the relationship between signal strength and position, these networks model the relationship between a position from trilateration and the localizing device's true position. However, adding a model of a moving device's likely transitions from position to position simply requires repeating the current model for each time step in a series, and describing the transitions between positions. This transition model is generated by linking one set of positional nodes with the positional nodes that directly follow the preceding nodes in time.

As well, there is the process of marginalizing any of the nodes in a Bayesian network. The typical structure of a HMM has only one state node and one observation node for each represented slice of time. One option in creating a temporal model is as described, where a larger network is simply repeated. However, the information contained in the CPTs of one node can be combined with the information contained in the CPTs of other nodes. For example, in the network presented in Figure 3.1, the child node C could be marginalized such that the network only contains nodes A and B. This is because

$$\mathrm{P}(C, A, B) = \mathrm{P}(C \mid A, B) \times \mathrm{P}(A \mid B) \times \mathrm{P}(B) \tag{5.3}$$

(which is the same as Equation 3.3), and because

$$\mathrm{P}(A, B) = \sum_{c \in C} \mathrm{P}(C \mid A, B) \times \mathrm{P}(A \mid B) \times \mathrm{P}(B) \tag{5.4}$$

in the network that contains all of A, B, and C. However, Equation 5.4 is also the expression for the joint distribution of A and B alone. The joint distribution for a network of only A and B is therefore calculable from the joint distribution of A, B, and C. This process of marginalizing individual nodes allows one to compile a larger network into a smaller one, such that my model described in this thesis document could be compiled to that of a single slice of a traditional HMM with only a state node and an observation node.

Given either of these two methods of converting my model into a temporal one, I can still extend the tactic of encoding more information in a model than other systems that apply Bayesian approaches. In specific, I could potentially bias the transition model based on maps of the environment. A common motion model, such as the motion model used by Raghavan et al. [38], describes a device moving from one position to anywhere within a normal distribution of the first position. The assumed possible speeds of the moving device are encoded as the standard deviation of the normal distribution. This does not account for any obstacles in the environment that represent positions in the environment that the localizing device could neither occupy nor pass through. Without a map built into the motion model, the system has the potential to think that a localizing device traveled through a wall that was narrow enough to be within the normal distribution about the original point. On the other hand, a map could be incorporated as a set of positions in the environment that the localizing device cannot occupy. As well, as with all variables in a Bayesian network, a node's parents determine its CPT: the position at time t_i is expressed as a probability given the position at time t_{i-1}. Therefore, it is possible to express the position at time t_i as less likely given the position at time t_{i-1}, if the shortest path between the two positions, including travel around any obstacles, would be unlikely given the assumed possible speeds of the device.

5.4.4 Including Multiple Signal Strength Readings

As mentioned, closed-form calibrations with a fixed set of parameters can be particularly prone to the sampling error of taking an individual signal strength reading, and attempting to translate directly to a specific distance. A probabilistic calibration for distance versus signal strength is only one way that modelling with Bayesian network allows one to overcome this.

In other BT localization systems, multiple signal strength readings could be incorporated with some kind of averaging, either by averaging the signal strength readings or by averaging the positions resulting from repeated localization, or some other combination. Otherwise, all but one reading would need to be discarded. But a Bayesian network model can also allow one to easily incorporate the information held in multiple signal strength readings, without any significant modelling or algorithmic changes.

This is achieved by simply adding more RSSI nodes to the net, with exactly the same distance and impedance model parent nodes. In a Bayesian network, because nodes' CPTs are defined in terms of the probability of values of that node, conditioned on values of its parents, additional RSSI nodes with the same distance and impedance model as parents would have identical CPTs–they would contain identical calibration with no additional calibration costs. As well, none of the structure or prior distributions of the rest of the model would have to change. However, if multiple RSSI nodes have evidence entered as part of a query for the joint distribution of the position of the localizing device, they will all influence the distribution of their parent distance, which in turn influences the estimated position of the localizing device. More importantly, if three readings are taken, and one reading was erroneous such that it could be interpreted as a number of possible distances, the other two readings that might point to one specific distance would outweigh the influence of the erroneous one. In this way, the automated reasoning power of a Bayesian network could accomplish a significant amount of signal processing that would otherwise have to be implemented separately.

In the models used in this thesis document, three signal strength readings per beacon was used as a default value, but was never varied experimentally. Experiments could be performed to compare the effect of the number of signal strength readings per beacon to the accuracy of localization. In particular, the results of using all of the chosen number of signal strength readings could be compared against the results when a selection method was used to reduce the number of signal strength readings to only one reading, as would necessarily be performed in a non-probabilistic system.

5.5 Summary

In this thesis document, I have described how I used Bayesian networks with discrete variables to model trilateration with iMacs as BT beacons. In §3.4, I also described how I modelled the relative orientation of iMacs, because of the effects that different parts of the iMac cases can have on BT signal propagation. In Chapter 4, I then described how I used this model to study a number of the issues involved in indoor localization using BT beacons for trilateration.

In specific, I undertook experiments to determine whether using discrete variables affected the accuracy of my model. I shifted the position of iMacs within the represented space such that they were at different locations within discrete spatial bins; I then repeatedly simulated localization, to find that the position of iMacs within the spatial bins did not affect the accuracy of localization. I also shifted the position of iMacs 2 m at a time so that the iMacs approached the boundaries of the represented space; after repeatedly simulating localization again, I found that as the iMacs progressed towards the edges of the space, the accuracy of localization decreased.

I also studied the effects on localization accuracy of the number of beacons and the number of distance calibration levels. I again simulated localization a number of times, varying the number of beacons used from zero to eight; and demonstrated that localization accuracy can increase when more beacons are used, but does not significantly decrease when fewer beacons are used. I also compared localization using default distance values with using twice as many values, and where one values was lower than the previous smallest distance value, and found that this increased localization accuracy at some spatial scales.

These results are significant to the field of indoor localization in a number of ways. As mentioned previously, only Blumrosen et al. [9] have rigorously performed calibration for BT trilateration at distances below 1 m; only Fernandez et al. [15] have studied the effect of varying the number of BT beacons used in trilateration, but only for 3 and 4 beacons; and only Bahl and Padmanabhan [5] and Cheung et al. [11] have explored the orientation of beacons on the propagation of BT signal. Because of their underrepresentation in the literature, the variations studied here have the potential to improve BT trilateration in general, when not applied to iMacs.

More importantly, the effects I have demonstrated have the potential to improve indoor localization accuracy outside of BT trilateration. The principles of BT trilateration and WLAN trilateration are similar, and variations such as the number of beacons or the distance calibration levels would likely have similar effects to WLAN trilateration. As well, I described in §2.3 how probabilistic temporal tracking techniques often make use of the results of separate closed-form trilateration phase, combining the information in a Markov chain. If these tracking systems were to incorporate any of the improvements described herein, to either the separate trilateration phase or by expanding the model of each time step of the Markov chain to include probabilistic trilateration calibration, the accuracy of the overall tracking process would undoubtedly also improve. Indoor localization systems would then continue to improve their utility to indoor location-based services, and continue to be viable alternatives to GPS and other outdoor localization systems.

References

[1] F Agostaro, F Collura, A Genco, and S Sorce. Problems and solutions in setting up a low-cost Bluetooth positioning system. *WSEAS Transactions on Computers*, 3:1102–1106, 2004.

[2] Varun Almaula and David Cheng. Bluetooth Triangulator. *Final Project, Department of Computer Science and Engineering, University of California, San Diego*, pages 1–5, 2006.

[3] S. Aparicio, J. Perez, A.M. Bernardos, and J.R. Casar. A fusion method based on bluetooth and WLAN technologies for indoor location. In *Multisensor Fusion and Integration for Intelligent Systems, IEEE International Conference on*, pages 487–491, 2008.

[4] Sofía Aparicio, Javier Pérez, P. Tarrío, Ana M. Bernardos, and José R. Casar. An Indoor Location Method Based on a Fusion Map Using Bluetooth and WLAN Technologies. In *International Symposium on Distributed Computing and Artificial Intelligence 2008 (DCAI 2008)*, volume 50, pages 702–710, 2009.

[5] P. Bahl and V.N. Padmanabhan. RADAR: an in-building RF-based user location and tracking system. In *INFOCOM 2000. Nineteenth Annual Joint Conference of the IEEE Computer and Communications Societies. Proceedings. IEEE*, volume 2, pages 775–784, 2000.

[6] U. Bandara, M. Hasegawa, M. Inoue, H. Morikawa, and T. Aoyama. Design and implementation of a Bluetooth signal strength based location sensing system. In *Radio and Wireless Conference, 2004 IEEE*, pages 319–322, 2004.

[7] R Bill, C Cap, M Kofahl, and T Mundt. Indoor and Outdoor Positioning in Mobile Environments: Review and some Investigations on WLAN-Positioning. *Geographic Information Sciences*, 10:91–98, 2004.

[8] J. Biswas and M. Veloso. WiFi localization and navigation for autonomous indoor mobile robots. In *Robotics and Automation (ICRA), 2010 IEEE International Conference on*, pages 4379–4384, 2010.

[9] Gaddi Blumrosen, Bracha Hod, Tal Anker, Danny Dolev, and Boris Rubinsky. Continuous Close-Proximity RSSI-Based Tracking in Wireless Sensor Networks. In *Body Sensor Networks (BSN), 2010 International Conference on*, pages 234–239, 2010.

[10] Zhe Chen. Bayesian Filtering: from Kalman filters to Particle filters, and Beyond. `http://www.damas.ift.ulaval.ca/_seminar/filesA11/10.1.1.107.7415.pdf`, 2003. Accessed on 26th of August, 2012.

[11] Kenneth C. Cheung, Stephen S. Intille, and Kent Larson. An Inexpensive Bluetooth-Based Indoor Positioning Hack. In *UbiComp 2006: Proceedings of the 8th International Conference on Ubiquitous Computing, Extended Abstracts*, 2006.

[12] S.Y. Cho. Localization of the arbitrary deployed APs for indoor wireless location-based applications. *Consumer Electronics, IEEE Transactions on*, 56:532–539, 2010.

[13] Rina Dechter. Bucket elimination: A unifying framework for reasoning. *Artificial Intelligence*, 113:41–85, 1999.

[14] Silke Feldmann, Kyandoghere Kyamakya, Ana Zapater, and Zighuo Lue. An indoor Bluetooth-based positioning system: concept, implementation and experimental evaluation. In *Proceedings of the International Conference on Wireless Networks, ICWN*, 2003.

[15] T.M. Fernandez, J. Rodas, C.J. Escudero, and D.I. Iglesia. Bluetooth Sensor Network Positioning System with Dynamic Calibration. In *Wireless Communication Systems, 4th International Symposium on*, pages 45–49, 2007.

[16] Julio Filho, Ana Bunoza, Jürgen Sommer, and Wolfgang Rosenstiel. Self-Localization in a Low Cost Bluetooth Environment. In *Ubiquitous Intelligence and Computing*, volume 5061, pages 258–270. Springer Berlin / Heidelberg, 2008.

[17] F. Forno, G. Malnati, and G. Portelli. Design and implementation of a Bluetooth ad hoc network for indoor positioning. *Software, IEE Proceedings on*, 152:223–228, 2005.

[18] Dieter Fox, Jeffrey Hightower, Henry Kauz, Lin Liao, and Don Patterson. Bayesian techniques for location estimation. In *Proceedings of The 2003 Workshop on Location-Aware Computing*, pages 16–18, 2003.

[19] J.E. Guivant and E.M. Nebot. Optimization of the simultaneous localization and map-building algorithm for real-time implementation. *Robotics and Automation, IEEE Transactions on*, 17:242–257, 2001.

[20] Youngjune Gwon, R. Jain, and T. Kawahara. Robust indoor location estimation of stationary and mobile users. In *INFOCOM 2004. Twenty-third Annual Joint Conference of the IEEE Computer and Communications Societies*, volume 2, pages 1032–1043, 2004.

[21] Andreas Haeberlen, Eliot Flannery, Andrew M. Ladd, Algis Rudys, Dan S. Wallach, and Lydia E. Kavraki. Practical robust localization over large-scale 802.11 wireless networks. In *Proceedings of the 10th annual international conference on Mobile computing and networking*, pages 70–84, 2004.

[22] Mohammad S. Hashemian, Kevin G. Stanley, and Nathaniel Osgood. Flunet: Automated tracking of contacts during flu season. In *Modeling and Optimization in Mobile, Ad Hoc and Wireless Networks (WiOpt), Proceedings of the 8th International Symposium on*, pages 348–353, 2010.

[23] Simon Hay and Robert Harle. Bluetooth Tracking without Discoverability. In *Location and Context Awareness*, volume 5561, pages 120–137. Springer Berlin / Heidelberg, 2009.

[24] J. Hightower and G. Borriello. Location systems for ubiquitous computing. *Computer*, 34:57–66, 2001.

[25] Andrew Howard, Sajid Siddiqi, and and Sukhatme. An Experimental Study of Localization Using Wireless Ethernet. In *Field and Service Robotics*, volume 24, pages 145–153. Springer Berlin / Heidelberg, 2006.

[26] A. Kotanen, M. Hännikäinen, H. Leppäkoski, and T.D. Hämäläinen. Experiments on local positioning with Bluetooth. In *Information Technology: Coding and Computing [Computers and Communications], Proceedings of the International Conference on*, pages 297–303, 2003.

[27] J. Kumagai and S. Cherry. Sensors and sensibility. *Spectrum, IEEE*, 41:22–26, 28, 2004.

[28] Erin-Ee-Lin Lau and Wan-Young Chung. Enhanced RSSI-Based Real-Time User Location Tracking System for Indoor and Outdoor Environments. In *Convergence Information Technology, International Conference on*, pages 1213–1218, 2007.

[29] S. L. Lauritzen and D. J. Spiegelhalter. Local Computations with Probabilities on Graphical Structures and Their Application to Expert Systems. *Journal of the Royal Statistical Society, Series B (Methodological)*, 50, 1988.

[30] Hui Liu, H. Darabi, P. Banerjee, and Jing Liu. Survey of Wireless Indoor Positioning Techniques and Systems. *Systems, Man, and Cybernetics, Part C: Applications and Reviews, IEEE Transactions on*, 37:1067–1080, 2007.

[31] Davide Macagnano and Giuseppe Thadeu Freitas de Abreu. Tracking Multiple Targets with Multidimensional Scaling. In *Proceedings of the 9th International Symposium on Wireless Personal Multimedia Communications*, 2006.

[32] F. Naya, H. Noma, R. Ohmura, and K. Kogure. Bluetooth-based indoor proximity sensing for nursing context awareness. In *Wearable Computers, Proceedings of the Ninth IEEE International Symposium on*, pages 212–213, 2005.

[33] Santosh Pandey and Prathima Agrawal. A survey on localization techniques for wireless networks. *Journal of the Chinese Institute of Engineers*, 29:1125–1148, 2006.

[34] Neal Patwari, Joshua N. Ash, Spyros Kyperountas, Alfred O. Hero III, Randolph L Moses, and Neieyr S. Correal. Locating the nodes: cooperative localization in wireless sensor networks. *Signal Processing Magazine, IEEE*, 22:54–69, 2005.

[35] J. Pearl. *Probabilistic Reasoning in Intelligent Systems: Networks of Plausible Inference*. Morgan Kaufmann series in representation and reasoning. Morgan Kaufmann Publishers, 1988.

[36] Ling Pei, Ruizhi Chen, Jingbin Liu, T. Tenhunen, H. Kuusniemi, and Yuwei Chen. Inquiry-Based Bluetooth Indoor Positioning via RSSI Probability Distributions. In *Advances in Satellite and Space Communications (SPACOMM), Second International Conference on*, pages 151–156, 2010.

[37] M. Rabinowitz and Jr. Spilker, J.J. A new positioning system using television synchronization signals. *Broadcasting, IEEE Transactions on*, 51:51–61, 2005.

[38] A.N. Raghavan, H. Ananthapadmanaban, M.S. Sivamurugan, and B. Ravindran. Accurate mobile robot localization in indoor environments using bluetooth. In *Robotics and Automation (ICRA), IEEE International Conference on*, pages 4391–4396, 2010.

[39] Teemu Roos, P. Myllymäki, Henry Tirri, Pauli Misikangas, and J. Sievänen. A Probabilistic Approach to WLAN User Location Estimation. *International Journal of Wireless Information Networks*, 9:155–164, 2002.

[40] Montserrat Ros, Joshua Boom, Gavin de Hosson, and Mathhew D'Souze. Indoor Localisation Using a Context-Aware Dynamic Position Tracking Model. *International Journal of Navigation and Observation*, 2012, 2012.

[41] Stuart J. Russell and Peter Norvig. *Artificial Intelligence: A Modern Approach*. Prentice Hall, 3 edition, 2011.

[42] Gaurav S. Sukhatme Sajid M. Saddiqi and Andrew Howard. Experiments in Monte-Carlo Localization using WiFi Signal Strength, 2003.

[43] Oscar Serrano, José María Cañas, Vicente Matellán, and Luis Rodero. Robot localization using WiFi signal without intensity map, 2004.

[44] V. Seshadri, G.V. Zaruba, and M. Huber. A Bayesian sampling approach to in-door localization of wireless devices using received signal strength indication. In *Pervasive Computing and Communications (PerCom), Third IEEE International Conference on*, pages 75–84, 2005.

[45] Ross D. Shachter. Evaluating influence diagrams. *OR*, 34:871–882, 1986.

[46] Adam Smith, Hari Balakrishnan, Michel Goraczko, and Nissanka Priyantha. Tracking moving devices with the cricket location system. In *Mobile systems, applications, and services, Proceedings of the 2nd international conference on*, pages 190–202, 2004.

[47] Andrew Symington and Niki Trigoni. Encounter based sensor tracking. In *Mobile Ad Hoc Networking and Computing, Proceedings of the thirteenth ACM international symposium on,*, pages 15–24, 2012.

[48] Sebastian Thrun. Bayesian Landmark Learning for Mobile Robot Localization. *Machine Learning*, 33:41–76, 1998.

[49] Sebastian Thrun, Dieter Fox, Wolfram Burgard, and Frank Dellaert. Robust monte carlo localization for mobile robots. *Artificial Intelligence*, 128:99–141, 2001.

[50] Frede Aakmann Tøgersen, Flemming Skjøth, Lene Munksgaard, and Søren Højsgaard. Wireless indoor tracking network based on kalman filters with an application to monitoring dairy cows. *Computers and Electronics in Agriculture*, 72:119–126, 2010.

[51] Jorge Torres-Solis, Tiago H. Falk, and Tom Chau. *A review of indoor localization technologies: towards navigational assistance for topographical disorientation*, chapter 3, pages 51–84. InTech, 2010.

[52] G. V. Zàruba, M. Huber, F. A. Kamangar, and I. Chlamtac. Indoor location tracking using RSSI readings from a single Wi-Fi access point. *Wireless Networks*, 13:221–235, 2007.